Supporting Information

A thiolated copper-hydride nanocluster with chloride bridging as a catalyst for carbonylative C– N coupling of aryl amines under mild conditions: a combined experimental and theoretical study

Anish Kumar Das, [a]‡ Sourav Biswas, [a]‡ Amit Pal, [a] Surya Sekhar Manna, [b] Avirup Sardar, [a] Pradip Kumar Mondal, [c] Basudev Sahoo,*[a] Biswarup Pathak,*[b] and Sukhendu Mandal *[a]

[a]School of Chemistry, Indian Institute of Science Education and Research Thiruvananthapuram, Kerala 695551, India. E-mail: sukhendu@iisertvm.ac.in

[b] Department of Chemistry, Indian Institute of Technology Indore, Madhya Pradesh 453552, India

[c] Elettra-Sincrotrone Trieste, S.S. 14 Km 163.5 in Area Science Park, Basovizza, Italy

‡These authors contributed equally.

Table of contents

Experimental

Materials

Tetrakis(acetonitrile)copper(I) tetrafluoroborate $Cu(CH_3CN)_4.BF_4$, triphenylphosphine (PPh_3), tert-butylthiol (HS^tBu), sodium borohydride ($NaBH_4$), sodium borodeuteride ($NaBD_4$) were procured from Sigma-Aldrich. All the reagents used for the catalysis reaction were also obtained from Sigma-Aldrich. HPLC grade solvents- chloroform, acetonitrile, methanol, and n-hexane were purchased from Spectrochem. Milli-Q water was utilized throughout the experiments.

Synthesis of $[Cu_{29}(S^tBu)_{12}(PPh_3)_4Cl_6H_{10}][BF_4]$ NC

Initially, 50 mg (0.16 mmol) of $Cu(CH_3CN)_4BF_4$ and 50 mg (0.19 mmol) of PPh_3 were mixed in the mixture solution of 2 mL acetonitrile and 0.5 mL chloroform at room temperature and stirred until a clear solution was obtained. After that, 14 μL (0.12 mmol) of HS^tBu was added to the mixture and continued stirring. After 15 min of stirring, 50 mg (1.32 mmol) of $NaBH_4$ dissolved in 2.5 mL methanol was added into the mixture, and a red color solution was formed. Then the reaction was kept for another 1 h under continuous stirring. After completion, the reaction mixture was centrifuged, and the red precipitate was formed. After drying properly, the precipitate was dissolved in the solvent mixture of chloroform/hexane (volume ratio 1:1). The final clear solution was kept for crystallization at ambient conditions. After 7 days, red-colored plate-like crystals were obtained.

Synthesis of $[Cu_{29}(S^tBu)_{12}(PPh_3)_4Cl_6D_{10}]^+$ ($Cu_{29}D$) NC

The same procedure was adopted, whatever was mentioned for the synthesis of the Cu_{29} NC. Instead of $NaBH_4$, we have used $NaBD_4$ as a reducing agent.

The general procedure of the catalytic reactions: Cu_{29}-nanocluster catalyzed carbamate formation from substituted Anilines and Benzimidazole (GP 1)

In an oven-dried screw cap vial equipped with a Teflon-coated stirring bar, Aniline 1 (0.2 mmol, 1.0 equiv.), Dialkylazodicarboxylate (2) (0.4 mmol, 2.0 equiv.), Cu_{29}-nanocluster (0.46 μmol, 0.0023 equiv.) were dissolved in dry $CDCl_3$ (0.3 M) under an inert atmosphere. The

reaction mixture was stirred at room temperature for 3 h. The reaction was monitored by checking TLC, and upon completion, the reaction was quenched by adding water and extracted with dichloromethane. The combined organic layers were washed once again with water (5 mL), followed by brine (5 mL), and the solvents were removed under reduced pressure. The crude reaction mixture was purified by using flash column chromatography through silica gel (eluent: ethyl acetate/ petroleum ether) to afford pure product 3.

X-ray Crystallography details

Single-crystal data of red-colored plate-like Cu_{29} NC was collected on a Bruker Axs Kappa Apex II SCXRD (single crystal X-ray diffractometer) with CCD detector (MoKα radiation, λ= 0.71073 Å) at the temperature of 100 K. Using Olex2,[S1] the structure was solved with the SHELXT[S2] structure solution program using Intrinsic Phasing and refined with the SHELXL[S3] refinement package using Least Squares minimization. *PLATON* SQUEEZE[S4] was applied during the final refinements to remove density mess from randomly oriented solvent molecules. All non-hydrogen atoms were refined anisotropically and hydrogen atoms were (positioned geometrically) refined isotropically using an olex2.[S1] We have successfully assigned the position and the number of hydrides in the structure by cautious SCXRD measurements.

Note: The finding of the hydrides is really a challenge because of the high electron density around the copper core compared to the low electron density of the hydrides and the hydrides are almost transparent to X-rays.[S5]

Computational details

All the calculations of Cu_{29} NC were carried out using the Vienna ab Initio Simulation Package (VASP) with projector augmented wave (PAW) method.[S6-S9] Generalized gradient approximations of Perdew−Burke−Ernzerhof (GGA-PBE) was used for describing the exchange-correlation interactions. Γ-Point was used to sample the Brillouin zone. An energy convergence criterion of 10^{-5} eV and force convergence criteria of 0.05 eV were employed. The DFT-D3 method was used for treating dispersion interactions of Cu_{29} NC. Moreover, more than 10 Å vacuum has been added in all three directions to avoid any periodic image interactions. Climbing image nudged elastic band (CI-NEB) with six images and dimer method was used for transition state analysis. The transition state is confirmed by the presence of one and only imaginary frequency.

The time-dependent density functional theory (TDDFT) calculations of Cu_{29} NC involving 300 excited states are carried out using Gaussian 09 Package with B3LYP functional and 6-31G* basis set.[S10-S12] LANL2DZ effective core potential is used for Cu atom.[S13,S14] The ligands are simplified to methyl for reducing computational expenditure in the structural calculations. Chloroform solvent was used under the conductor-like polarizable continuum solvation model (CPCM).

Instrumentation

A SHIMADZU UV-3800 spectrometer was used for measuring the absorbance spectra. FEI Tecnai G2 F30 S -Twin transmission electron microscope (TEM) 300 kV, scanning electron microscope (SEM), and energy-dispersive X-ray spectroscopy (EDS; FEI Nova NANOSEM 450) were used for the microscopic characterization. X-ray photoelectron spectroscopy (XPS) measurement has been done by using the Omicron Nanotech instrument (MgK_{α} radiation at 1253.6 eV). All binding energies were referenced to the neutral C 1s peak at 284.8 eV. Bruker Avance III, 500 MHz, NMR was used for the ^{1}H, ^{11}B, ^{13}C, ^{19}F and ^{31}P studies. Waters Q-TOF mass spectrometer equipped with a Z-spray source was used for the electrospray ionization (ESI) mass spectrometry measurement in positive mode. Samples were dissolved in chloroform (1 mg/mL) and diluted by methanol (1:1). The solution was infused at 160 µL/min. The spectrometer was operated in the mass range of m/z 2000–10000, capillary voltage was 4.65 kV, sampling cone 80 V, source temperature 80 °C, source offset 28 V, desolvation temperature 150 °C, cone gas flow 179 L/Hr, desolvation gas flow 740 L/Hr. For the isolated catalyst, the parameters: capillary voltage 3.3 kV, sampling cone 60 V, source temperature 70 °C, source offset 10 V, desolvation temperature 400 °C, cone gas flow 50 L/Hr, desolvation gas flow 200 L/Hr.

Variation of Anilines

Isopropyl phenylcarbamate (3aa):

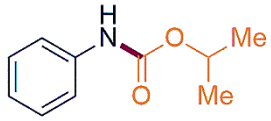

Following **GP 1**, the starting materials **1a** (0.2 mmol) and **2a** (0.4 mmol) afforded the compound **3aa**, as a white solid (25.4 mg, 0.142 mmol, 71%).

^{1}H NMR (500 MHz, $CDCl_3$) δ (ppm) = 7.37 (d, J = 7.7 Hz, 2H), 7.30 (t, J = 6.9 Hz, 2H), 7.05 (t, J = 7.3 Hz, 1H), 6.52 (s, 1H), 5.06-4.98 (m, 1H), 1.30 (d, J = 6.3 Hz, 6H); The spectroscopic data obtained were in agreement with the reported data for the compound **3aa**.[S15]

Isopropyl *p*-tolylcarbamate (3ba):

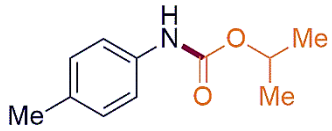

Following **GP1**, the starting materials **1b** (0.2 mmol) and **2a** (0.4 mmol) afforded the compound **3ba**, as a white solid (26.6 mg, 0.138 mmol, 69%).

^{1}H NMR (500 MHz, $CDCl_3$) δ (ppm) = 7.13 (d, J = 7.8 Hz, 2H), 7.10 (d, J = 8.6 Hz, 2H), 6.45 (s, 1H), 5.03-4.98 (m, 1H), 2.30 (s, 3H), 1.29 (d, J = 6.3 Hz, 6H); The spectroscopic data obtained were in agreement with the reported data for the compound **3ba**.[S15]

Isopropyl (4-(tert-butyl)phenyl)carbamate (3ca):

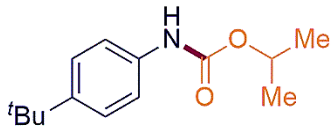

Following **GP1**, the starting materials **1c** (0.2 mmol) and **2a** (0.4 mmol) afforded the compound **3ca**, as a white solid (32 mg, 0.136 mmol, 68%).

^{1}H NMR (500 MHz, $CDCl_3$) δ (ppm) = 7.31-7.33 (m, 4H), 6.47 (s, 1H), 4.98-5.05 (m, 1H), 1.58 (s, 9H), 1.29 (d, J = 5.5 Hz, 6H).; The spectroscopic data obtained were in agreement with the reported data for the compound **3ca**.[S16]

Isopropyl (3,5-dimethylphenyl)carbamate (3da):

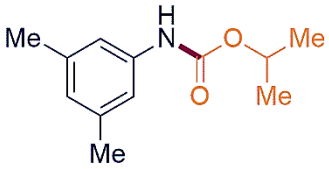

Following **GP1**, the starting materials **1d** (0.2 mmol) and **2a** (0.4 mmol) afforded the compound **3da**, as a colourless liquid (28.6 mg, 0.138 mmol, 69%).

^{1}H NMR (500 MHz, $CDCl_3$) δ (ppm) = 7.01 (s, 2H), 6.70 (s, 1H), 6.42 (s, 1H), 4.96-5.03 (m, 1H), 2.28 (s, 6H), 1.29 (d, J = 6.3 Hz, 6H); The spectroscopic data obtained were in agreement with the reported data for the compound **3da**.[S15]

Isopropyl (4-chlorophenyl)carbamate (3ea):

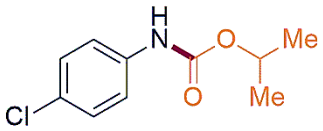

Following **GP1**, the starting materials **1e** (0.2 mmol) and **2a** (0.4 mmol) afforded the compound **3ea**, as a white solid (27.8 mg, 0.13 mmol, 65%).

^{1}H NMR (500 MHz, $CDCl_3$) δ (ppm) = 7.18 (d, J = 8.8 Hz, 2H), 7.16 (d, J = 8.8 Hz, 2H), 6.48 (s, 1H), 4.89-4.97 (m, 1H), 1.22 (d, J = 6.3 Hz, 6H); The spectroscopic data obtained were in agreement with the reported data for the compound **3ea**.[S15]

Isopropyl (4-bromophenyl)carbamate (3fa):

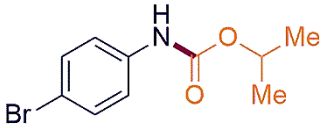

Following **GP1**, the starting materials **1f** (0.2 mmol) and **2a** (0.4 mmol) afforded the compound **3fa**, as a white solid (31.87 mg, 0.12 mmol, 62%).

^{1}H NMR (500 MHz, $CDCl_3$) δ (ppm) = 7.48 (d, J = 8.8 Hz, 2H), 7.39 (d, J = 8.8 Hz, 2H), 6.57 (s, 1H), 4.97-5.05 (m, 1H), 1.29 (d, J = 6.3 Hz, 6H); The spectroscopic data obtained were in agreement with the reported data for the compound **3fa**.[S15]

Isopropyl pyridin-2-ylcarbamate (3ga):

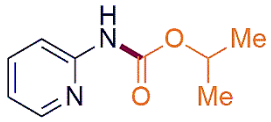

Following **GP1**, the starting materials **1g** (0.2 mmol) and **2a** (0.4 mmol) afforded the compound **3ga**, as a white solid (16.94 mg, 0.094 mmol, 47%).

^{1}H NMR (500 MHz, $CDCl_3$) δ (ppm) = 8.29 (s, 1H), 7.98 (d, J = 8.5 Hz, 1 H), 7.66-7.70 (m, 1H), 6.96-6.99 (m, 1H), 5.01-5.08 (m, 1H), 1.32 (d, J = 6.3 Hz, 6H); The spectroscopic data obtained were in agreement with the reported data for the compound **3ga**.[S15]

Variation of Dialkylazodicarboxylate

Ethyl phenylcarbamate (3ab):

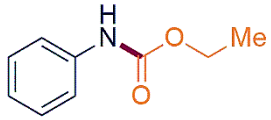

Following **GP1**, the starting materials **1a** (0.2 mmol) and **2b** (0.4 mmol) afforded the compound **3ab**, as a white solid (25.77 mg, 0.156 mmol, 78%).

^{1}H NMR (500 MHz, $CDCl_3$) δ (ppm) = 7.31 (d, J = 8.2 Hz, 2H), 7.23 (t, J = 7.9 Hz, 2H), 6.99 (t, J = 7.4 Hz, 1H), 6.52 (s, 1H), 4.13-4.18 (q, J = 7.2 Hz, 2H), 1.24 (t, J = 7.2 Hz, 3H); The spectroscopic data obtained were in agreement with the reported data for the compound **3ab**.[S17]

***tert*-butyl phenylcarbamate (3ac):**

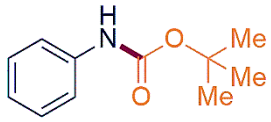

Following **GP1**, the starting materials **1a** (0.2 mmol) and **2c** (0.4 mmol) afforded the compound **3ac**, as a white solid (21.5 mg, 0.131 mmol, 65%).

^{1}H NMR (500 MHz, $CDCl_3$) δ (ppm) = 7.41 (d, J = 8.8 Hz, 2H), 7.29 (t, J = 8.4 Hz, 2H), 7.03 (t, J = 7.4 Hz, 1H), 6.46 (s, 1H), 1.52 (s, 9H); The spectroscopic data obtained were in agreement with the reported data for the compound **3ac**.[S18]

Variation of Benzimidazole

Isopropyl 1H-benzo[d]imidazole-1-carboxylate (4a):

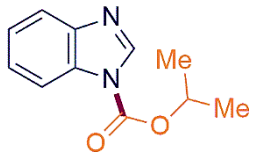

Following **GP1**, the starting materials Benzimidazole (0.2 mmol) and **2a** (0.4 mmol) afforded the compound **4a**, as a colourless liquid (26.94 mg, 0.132 mmol, 66%).

^{1}H NMR (500 MHz, $CDCl_3$) δ (ppm) = 8.48 (s, 1H), 8.03 (d, *J* = 7.8 Hz, 1H), 7.80 (d, *J* = 9.13 Hz, 1H), 7.35 – 7.42 (m, 2H), 5.30 – 5.37 (m, 1H), 1.50 (d, *J* = 6.3 Hz, 6H); **^{13}C NMR (126 MHz, $CDCl_3$)** δ (ppm) = 155.4, 149.2, 142.0, 125.5, 124.6, 120.8, 114.6, 73.0, 22.0; **HRMS (ESI):** m/z calc. for ($C_{14}H_{19}N_2O_2^+$) $[M+H]^+$: 205.0972; found: 205.0969; **IR (ATR) (ν cm^{-1}):** 1758, 1521, 1460, 1387, 1251, 1110.

Ethyl 1H-benzo[d]imidazole-1-carboxylate (4b):

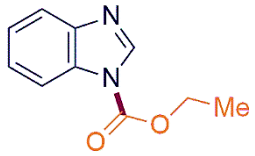

Following **GP 1**, the starting materials Benzimidazole (0.2 mmol) and **2b** (0.4 mmol) afforded the compound **4b**, as a white solid (27.77 mg, 0.146 mmol, 73%).

^{1}H NMR (500 MHz, $CDCl_3$) *δ* (ppm) = 8.47 (s, 1H), 8.02 (d, *J* = 7.7 Hz, 1H), 7.79 (d, *J* = 7.6 Hz, 1H), 7.35-7.42 (m, 2H), 4.54-4.58 (m, 2H), 1.51 (t, *J* = 6.3 Hz, 3H); The spectroscopic data obtained were in agreement with the reported data for the compound **4b**.[S15]

***tert*-butyl 1H-benzo[d]imidazole-1-carboxylate (4c):**

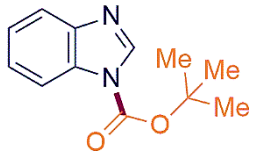

Following **GP1**, the starting materials Benzimidazole (0.2 mmol) and **2c** (0.4 mmol) afforded the compound **4c**, as a white solid (25.8 mg, 0.118 mmol, 59%).

^{1}H NMR (500 MHz, $CDCl_3$) δ (ppm) = δ (ppm) = 8.43 (s, 1H), 7.98 (d, J = 7.8 Hz, 1H), 7.78 (d J = 7.4 Hz, 1H), 7.39-7.33 (m, 2H), 1.69 (s, 9H); The spectroscopic data obtained were in agreement with the reported data for the compound **4c**.[S18]

Mechanistic Investigation

Radical Trapping Experiment with TEMPO:

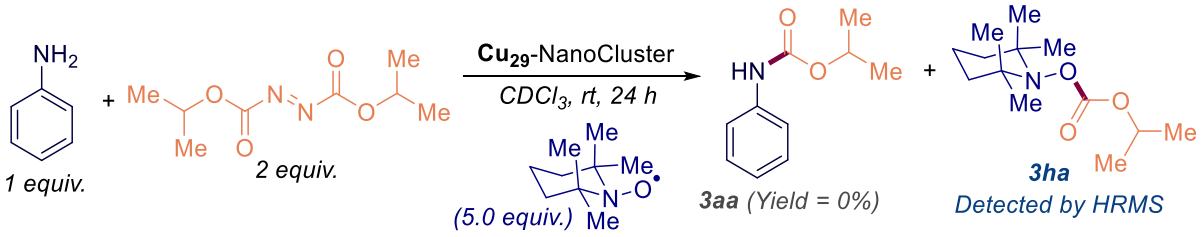

In an oven-dried screw cap vial equipped with a Teflon-coated stirring bar, Aniline **1** (0.2 mmol, 1.0 equiv.), Dialkylazodicarboxylate (**2**) (0.4 mmol, 2.0 equiv.), Cu_{29}-cluster (0.46 µmol, 0.0023 equiv.) and TEMPO (1 mmol, 5 equiv.) were dissolved in dry $CDCl_3$ (0.3 M) under inert atmosphere. The reaction mixture was stirred at room temperature for 3 h. The reaction was monitored by checking TLC and upon completion, the reaction was quenched by adding water and extracted with dichloromethane. The combined organic layers were washed once again with water (5 mL), followed by brine (5 mL) and the solvents were removed under reduced pressure. HRMS analysis of the crude reaction mixture identified Isopropyl (2,2,6,6-tetramethylpiperidin-1-yl) carbonate (Oxyacyl-TEMPO adduct) (**3ha**).

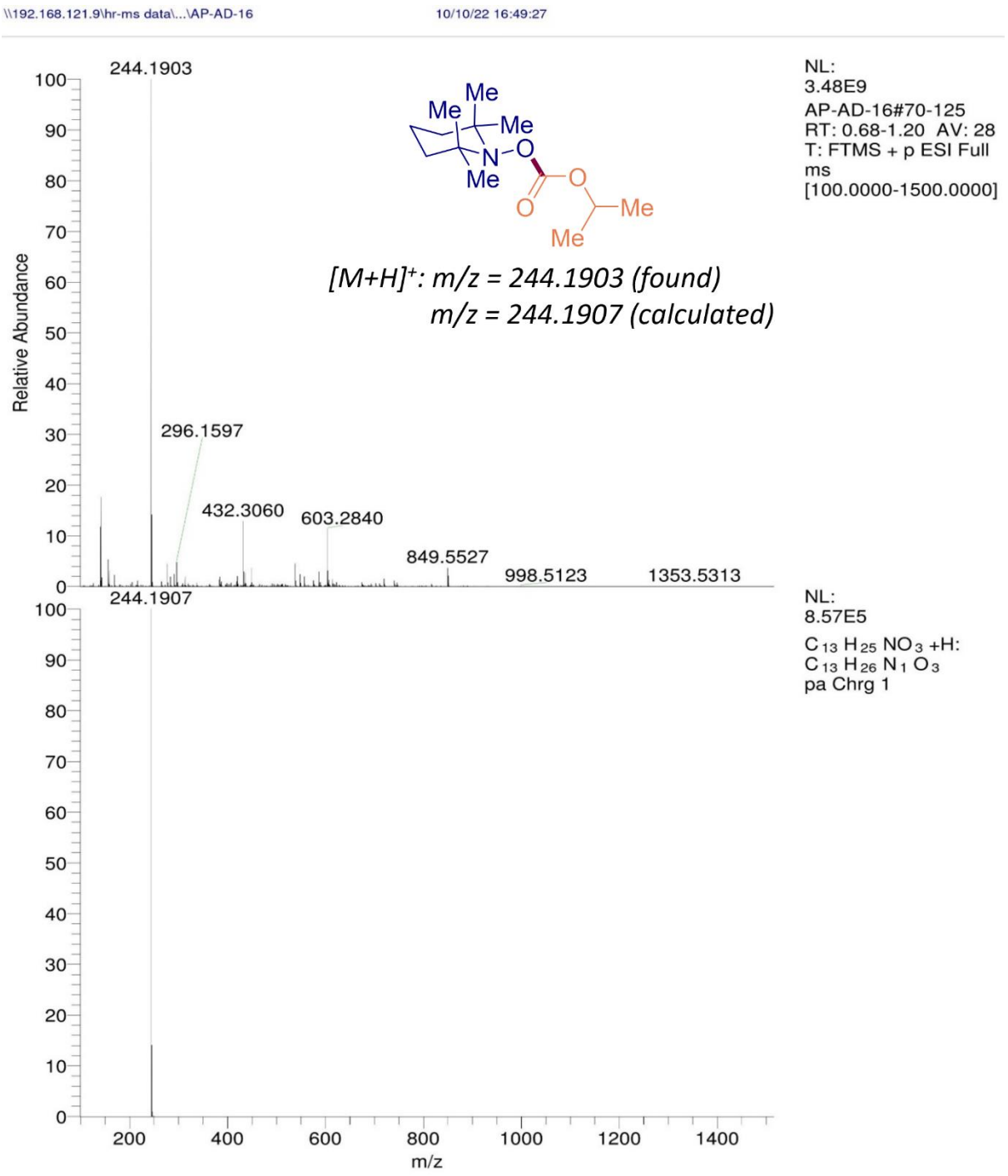

Detection of Isopropyl (2,2,6,6-tetramethylpiperidin-1-yl) carbonate (**3ha**) adduct in the crude reaction mixture of radical trapping experiment using TEMPO by HRMS analysis.

Radical Experiment with 1,1-diphenylethene:

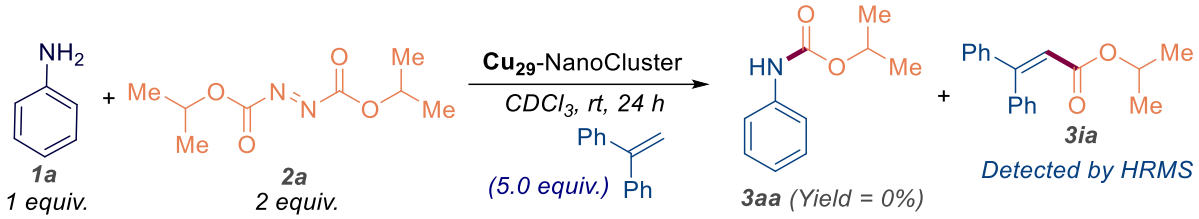

In an oven-dried screw cap vial equipped with a Teflon-coated stirring bar, Aniline **1** (0.2 mmol, 1.0 equiv.), Dialkylazodicarboxylate (**2**) (0.4 mmol, 2.0 equiv.), Cu_{29}-Cluster (0.46 µmol, 0.0023 equiv.) and 1,1-diphenylethene (1 mmol, 5 equiv.) were dissolved in dry $CDCl_3$ (0.3 M) under inert atmosphere. The reaction mixture was stirred at room temperature for 3 h. The reaction was monitored by checking TLC and upon completion, the reaction was quenched by adding water and extracted with dichloromethane. The combined organic layers were washed once again with water (5 mL), followed by brine (5 mL) and the solvents were removed under reduced pressure. HRMS analysis of the crude reaction mixture identified Isopropyl 3,3-diphenylacrylate (**3ia**).

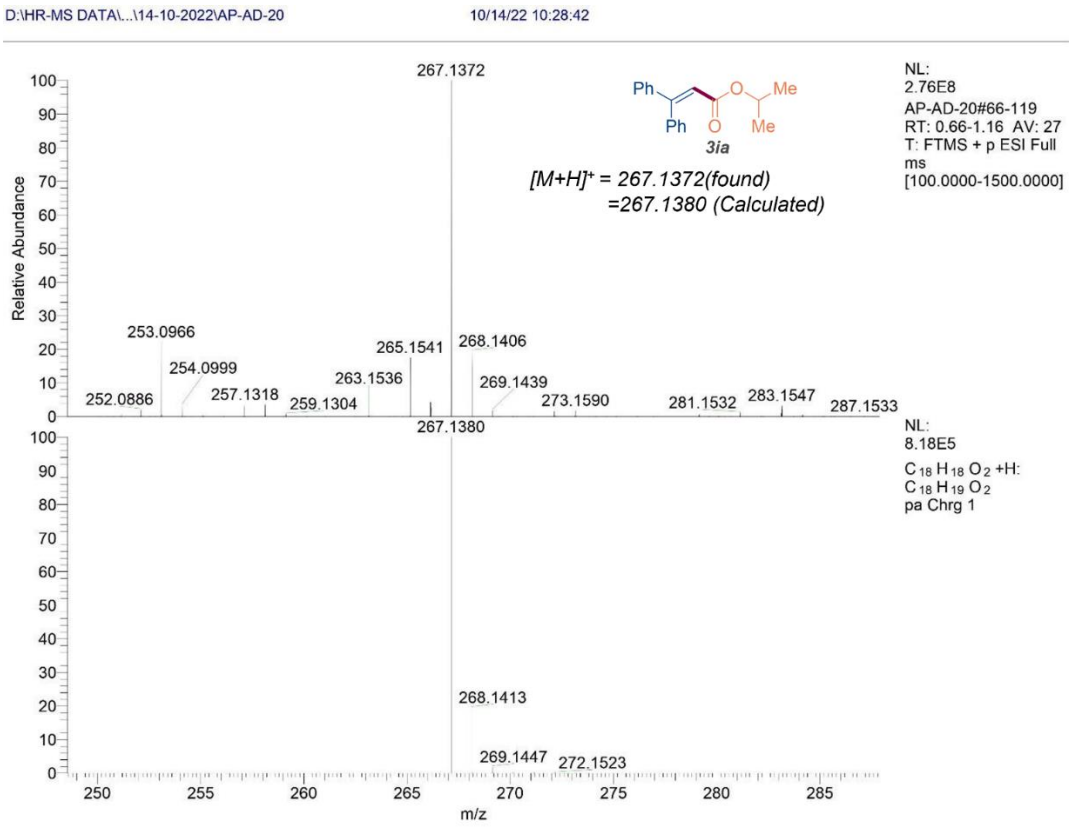

Detection of Isopropyl 3,3-diphenylacrylate (**3ia**) adduct in the crude reaction mixture of radical trapping experiment using 1,1-diphenylethene by HRMS analysis.

Control Experiments

Catalysis reaction without Cu_{29}-Nanocluster: In an oven-dried screw cap vial equipped with a Teflon-coated stirring bar, Aniline **1** (0.2 mmol, 1.0 equiv.), di-alkyl azodicarboxylate (**2**) (0.4 mmol, 2.0 equiv.) were dissolved in dry $CDCl_3$ (0.3 M) under inert atmosphere. The reaction mixture was stirred at room temperature for 3 h. The reaction was monitored by checking TLC and upon completion, the reaction was quenched by adding water and extracted with dichloromethane. The combined organic layers were washed once again with water (5 mL), followed by brine (5 mL) and the solvents were removed under reduced pressure. The crude reaction mixture was analysed by ^{1}H NMR using 1,3,5-trimethoxy benzene as an internal standard and no product formation had been identified.

Catalysis reaction with CuI: In an oven-dried screw cap vial equipped with a Teflon-coated stirring bar, Aniline **1** (0.2 mmol, 1.0 equiv.), di-alkyl azodicarboxylate (**2**) (0.4 mmol, 2.0 equiv.) CuI (21 μmol) were dissolved in dry $CDCl_3$ (0.3 M) under inert atmosphere. The reaction mixture was stirred at room temperature for 3 h. The reaction was monitored by checking TLC and upon completion, the reaction was quenched by adding water and extracted with dichloromethane. The combined organic layers were washed once again with water (5 mL), followed by brine (5 mL) and the solvents were removed under reduced pressure. The crude reaction mixture was analysed by ^{1}H NMR using 1,3,5-trimethoxy benzene as an internal standard and yield is 5%.

Catalyst regeneration: In an oven-dried screw cap vial equipped with a Teflon-coated stirring bar, 4-bromo aniline (1f) (0.2 mmol, 1.0 equiv.), diisopropyl azodicarboxylate (2a) (0.4 mmol, 2.0 equiv.), Cu_{29}-nanocluster (0.46 μmol, 0.0023 equiv.) were dissolved in dry $CDCl_3$ (0.3 M) under an inert atmosphere. The reaction mixture was stirred at room temperature for 3 h. The reaction was monitored by checking TLC, and upon completion, the reaction was quenched by adding water and extracted with dichloromethane. The combined organic layers were washed once again with water (5 mL), followed by brine (5 mL), and the solvents were removed under reduced pressure. The crude reaction mixture was washed with 20% ethyl acetate/ petroleum ether to remove all the organic compounds from the catalytic reaction mixture followed by the remaining crude was washed with distilled $CHCl_3$ to get back the Cu_{29} NC (catalyst) and organic crude was purified by using flash column chromatography through Silica gel (eluent: ethyl acetate/ petroleum ether) to afford pure product **3fa**.

N.B. Recovered Cu_{29} NC after the catalytic reaction was also well characterised by using ^{1}H NMR, mass Spectrometry and absorption studies.

Table S1. Crystal data and structure refinement parameters.

Identification code	Cu_{29} NC
Empirical formula	C_{243} H_{359} B_2 Cl_{21} Cu_{58} F_8 P_8 S_{24}
CCDC number	2242226
Formula weight	8900.87
Temperature/K	100(2)
Wavelength/Å	0.71073
Crystal system	Triclinic
Space group	*P*-1 (No. 2)
a/Å	24.596(5)
b/Å	28.305(6)
c/Å	29.247(6)
α/°	64.888(8)
β/°	81.085(9)
γ/°	81.878(9)
Volume/$Å^3$	18149(6)
Z	2
$\rho_{calc}g/cm^3$	1.629
μ/mm^{-1}	3.679
F(000)	8884
Crystal size/mm^3	0.095 × 0.048 × 0.028
2θ range for data collection/°	0.852 to 24.000
Index ranges	-28<=h<=28, -32<=k<=32, -33<=l<=33
Reflections collected	193059
Independent reflections	12945 [R(int) = 0.4288]
Data/restraints/parameters	56494 / 5490 / 3086
Goodness-of-fit on F^2	0.912
Final R indexes [I>=2σ (I)]	R_1 = 0.1233, wR_2 = 0.2983
Largest diff. peak/hole / e $Å^{-3}$	1.779 and -1.881

Table S2. Position of ten hydrides in the Cu_{29} NC.

Chemical shift (ppm)	Peaks integration	Hydrides identification in the structure
2.01	5	(i) 5 μ_3 bridged hydrides
2.17	1	(ii) 1 μ_3 bridged hydride
2.94	1	(iii) 1 μ_3 bridged hydride
3.01	1	(iv) 1 μ_3 bridged hydride
3.49 & 3.50	2	(v) 2 μ_5 bridged hydrides

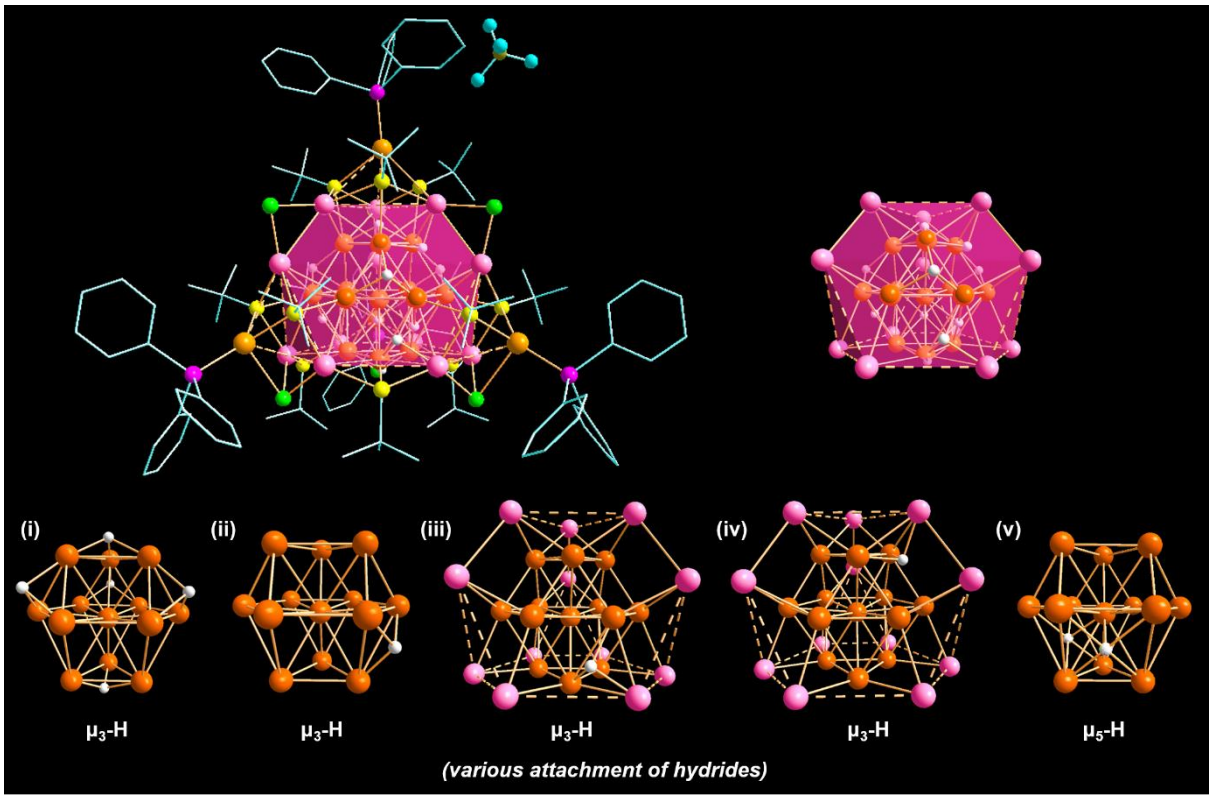

The total crystal structure of Cu_{29} NC with various hydride attachments. Color legend; Cu(core), deep orange; Cu(Cu_{12} shell), rose; Cu(Cu_4 shell), light orange; S, yellow; P, magenta; Cl, green; C, grey stick; B, dark yellow; F, turquoise; H, white. H atoms and solvent molecules are partially omitted for clarity.

Table S3. Theoretical insights into the mechanism of the catalysis reaction.

Step	Free energy change (eV)	Proposed reasons
a → b	-0.74 (exergonic)	H-bonding interaction (2.8-3.1 Å) between the Azo and Cl atoms of Cu_{29} NC
b → c	+2.58 (endergonic)	Electronic repulsion between the free radicals on the carbon atoms and the lone pairs on the Cl atoms in Cu_{29} NC
c → d	-0.61 (exergonic)	N-H bond of aniline approaching the carbonyl radical
d → TS → e	-0.48 (exergonic)	Formation of stable C-H σ-bond of carbonyl *via* H· transfer from aniline to carbonyl
e → f	-3.7 (exergonic)	Formation of the final stable carbamate compound

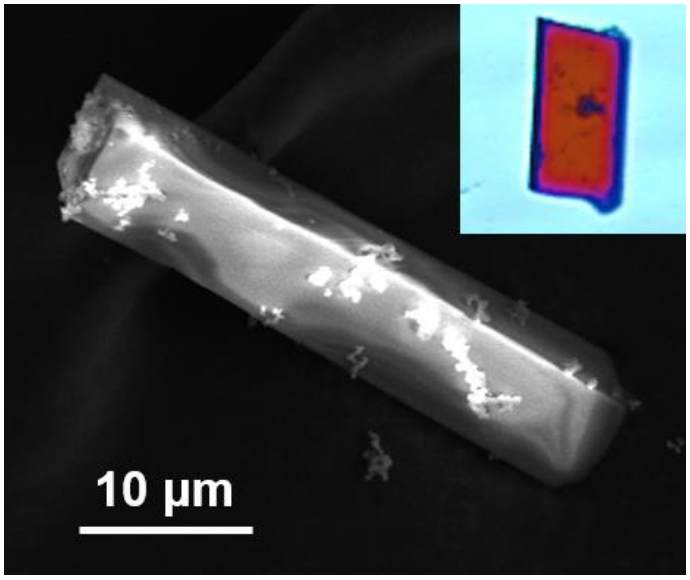

Fig. S1 SEM and optical microscope (inset) images of Cu_{29} crystal.

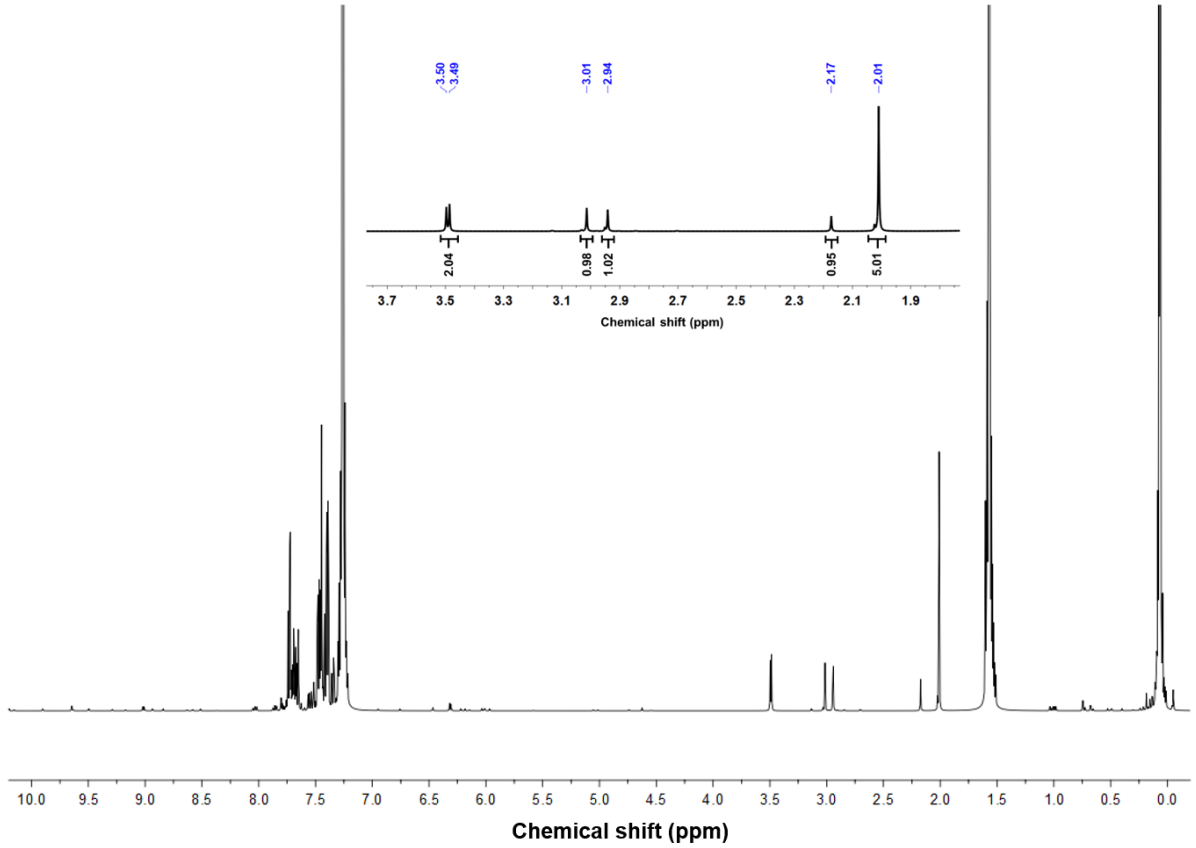

Fig. S2 ^{1}H NMR of Cu_{29} NC. A sharp peak at 1.569 ppm is associated with the proton of the *tert*-butyl group. A few more broad peaks are obtained in the aromatic proton region which originates from protons of the PPh_3 ligand. This broadening is attributed to more significant differences in the environments of the auxiliary ligands.[S5] Inset highlights the hydride region of the Cu_{29} NC.

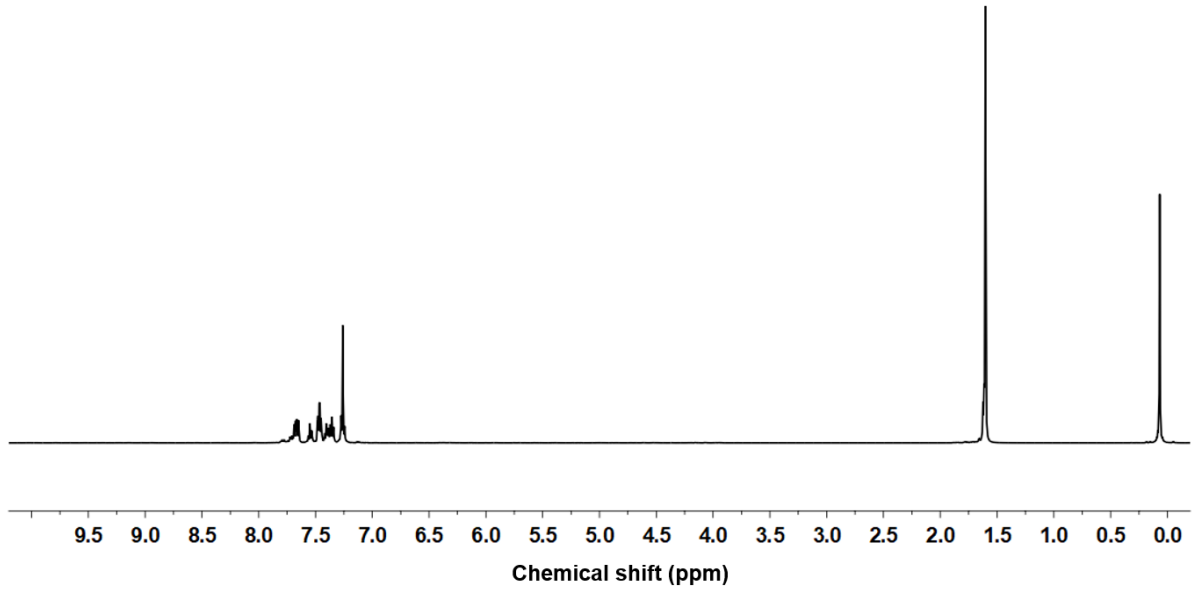

Fig. S3 The ^{1}H NMR of the Cu_{29}D NC.

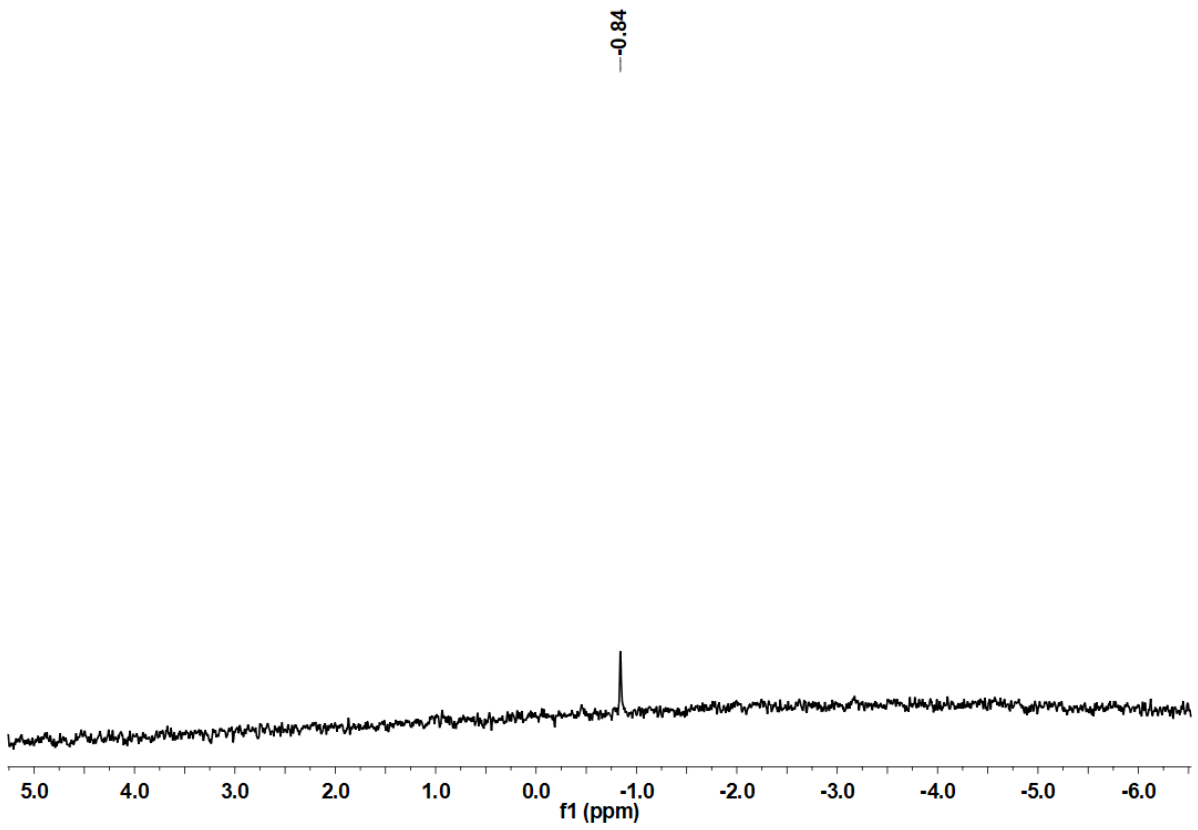

Fig. S4 ^{11}B NMR of Cu_{29} NC.

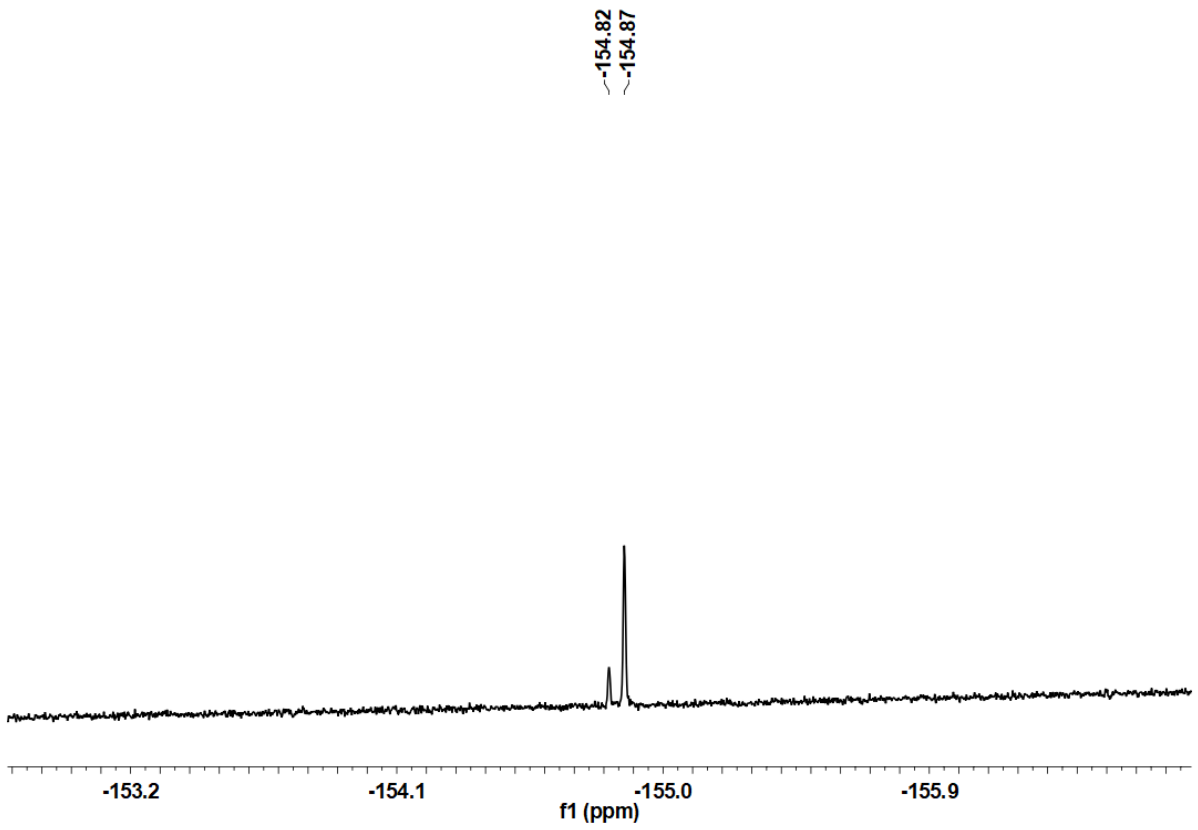

Fig. S5 ^{19}F NMR of Cu_{29} NC.

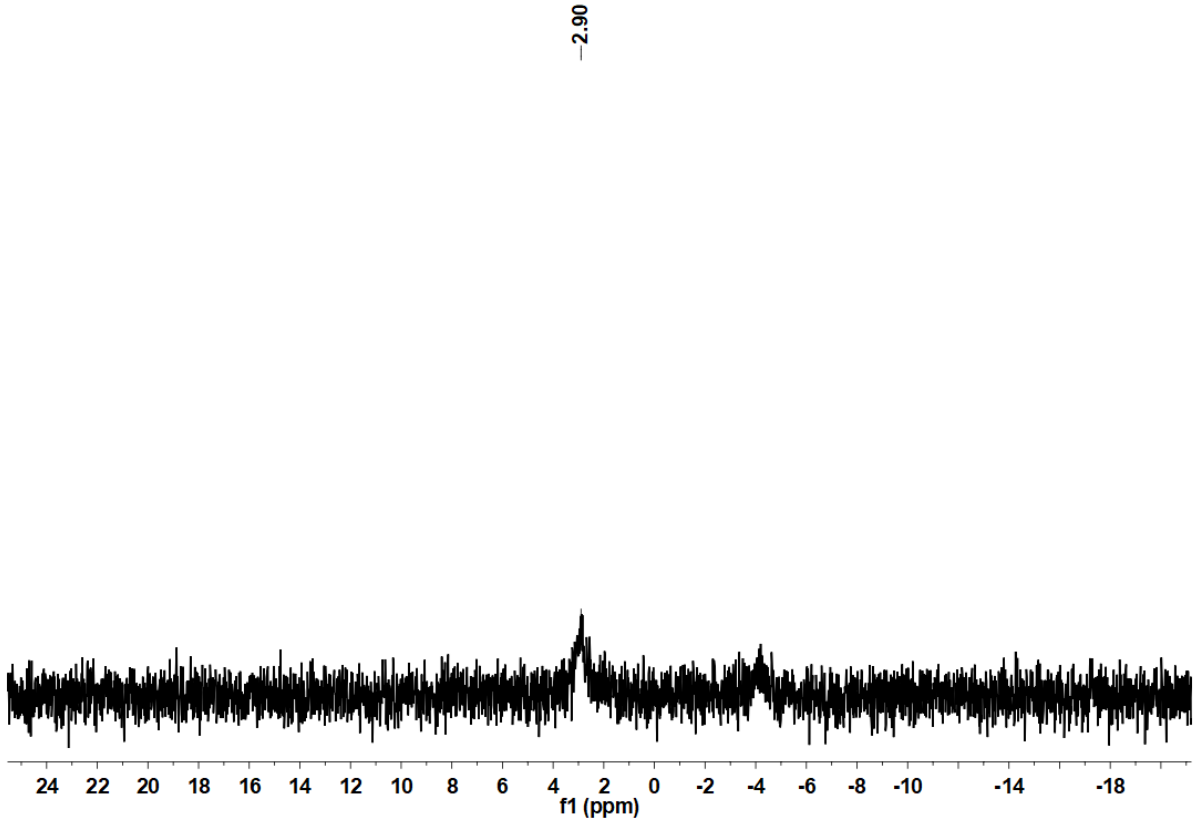

Fig. S6 ^{31}P NMR of Cu_{29} NC.

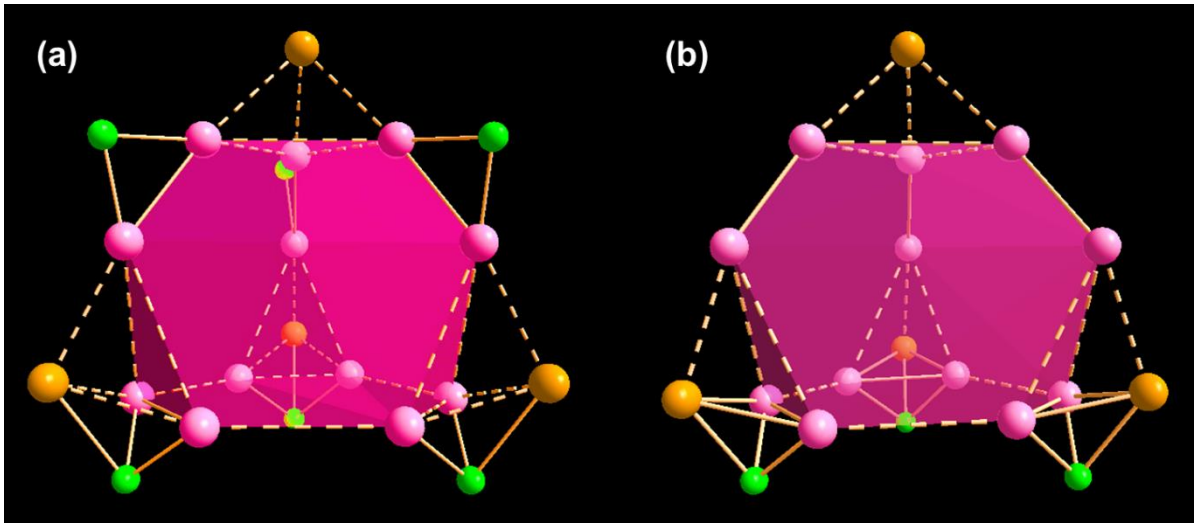

Fig. S7 (a) μ_2 and μ_3 bridging modes of Cl^- in the shell of the Cu_{29} NC, and (b) μ_3 bridging modes of Cl^- in the shell of the reported $[Cu_{29}(SAdm)_{15}Cl_3(P(Ph\text{-}Cl)_3)_4H_{10}]^+$ NC. Color legend; Cu(Cu_{12} shell), rose; Cu(Cu_4 shell), light orange; Cl, green.

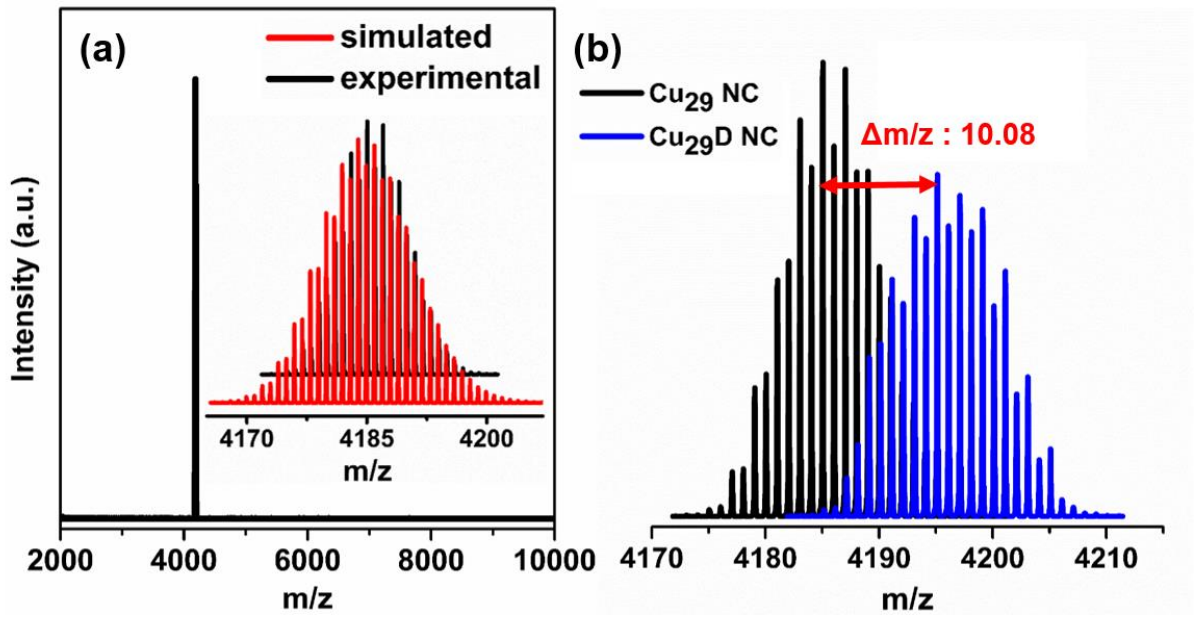

Fig. S8 (a) Positive mode ESI-MS spectrum of Cu_{29} NC. Inset showing the good agreement between the simulated and experimental isotopic patterns of the peak corresponding to $[Cu_{29}(S^tBu)_{12}(PPh_3)_4Cl_6H_{10}]^+$, and (b) the mass difference of the isotopic patterns between the Cu_{29} NC and Cu_{29}D NC.

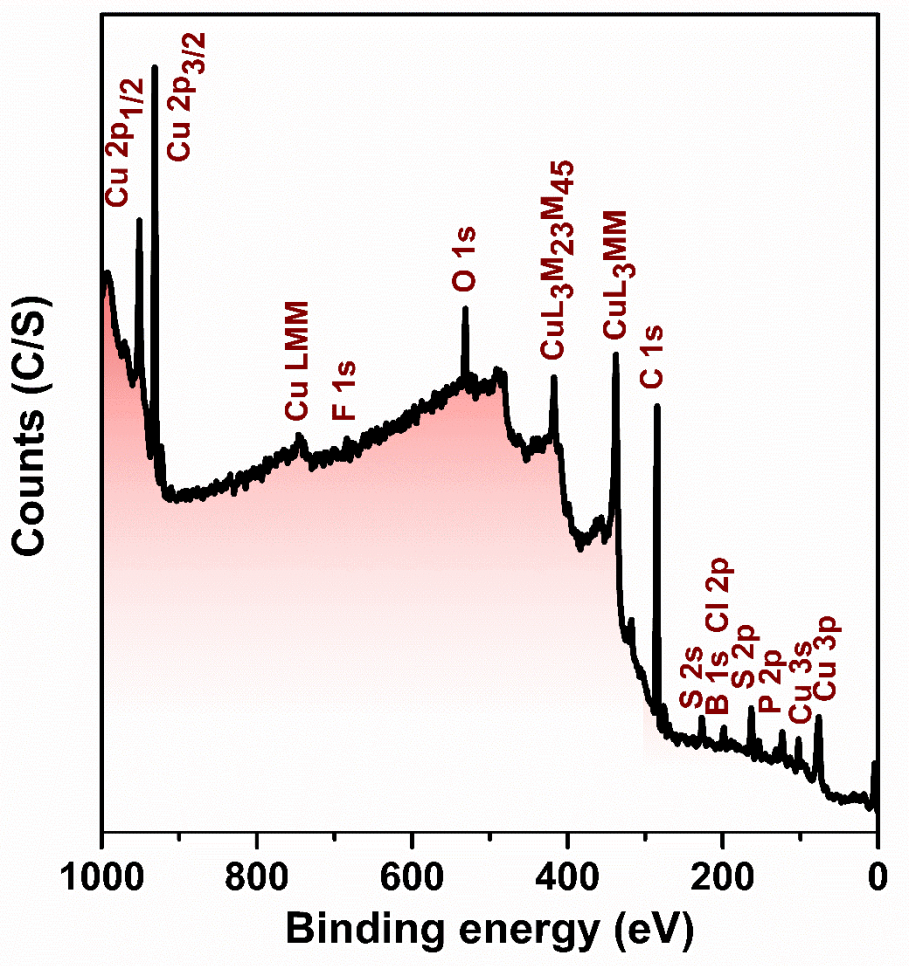

Fig. S9 XPS survey spectrum of Cu_{29} NC. The acquired XPS survey spectrum demonstrates the presence of all the necessary elements.

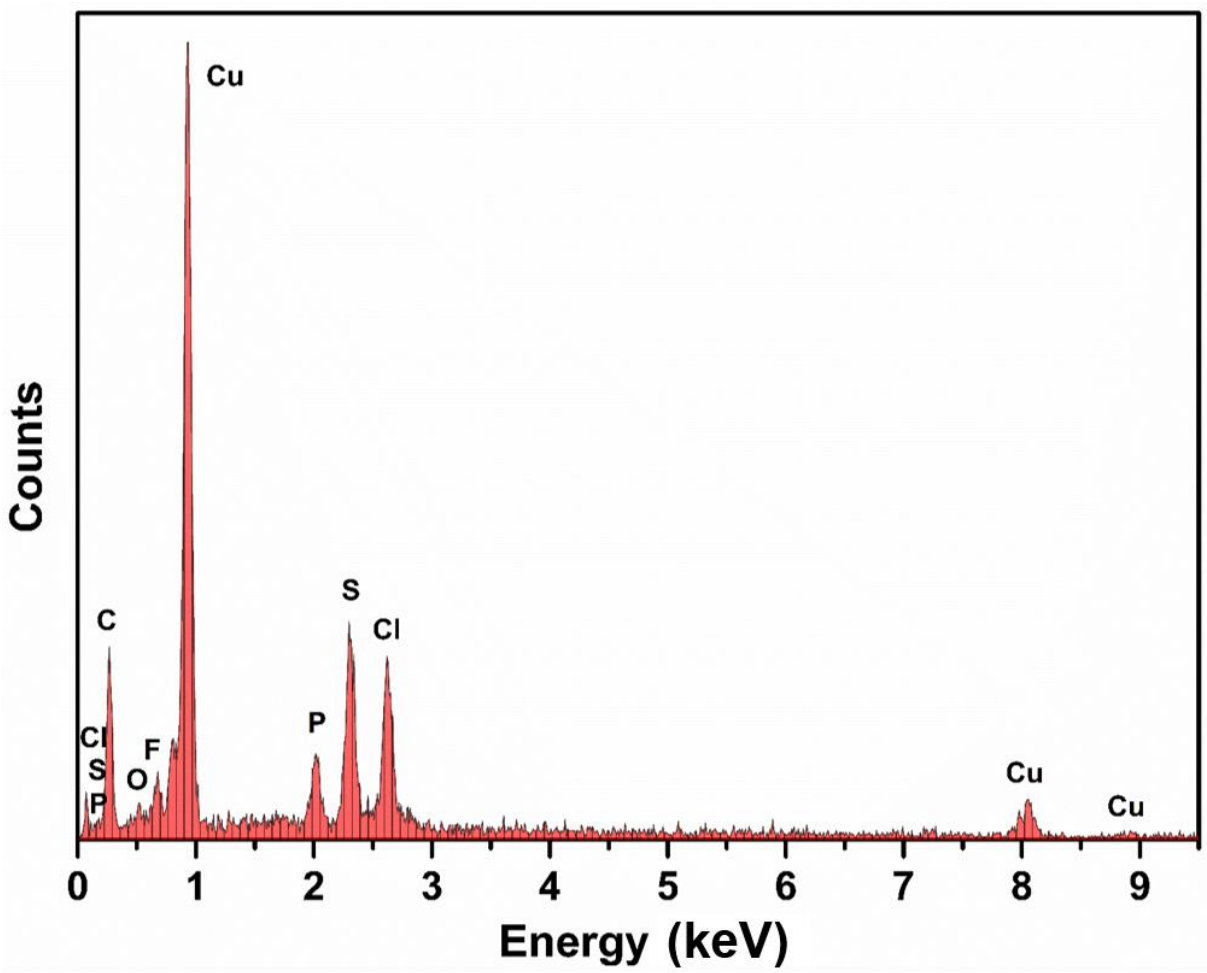

Fig. S10 Energy dispersive spectrum of Cu_{29} NC. The obtained result is also corroborated with the crystal structure by the elemental analysis.

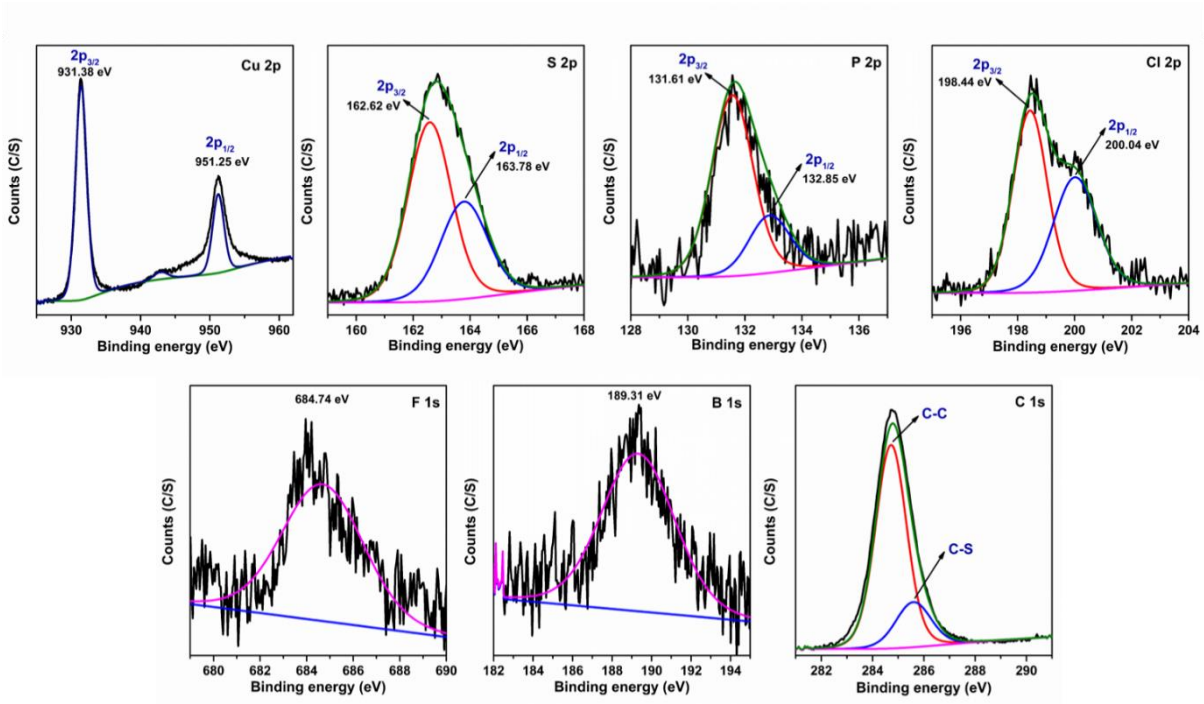

Fig. S11 High-resolution XPS spectra of each element.

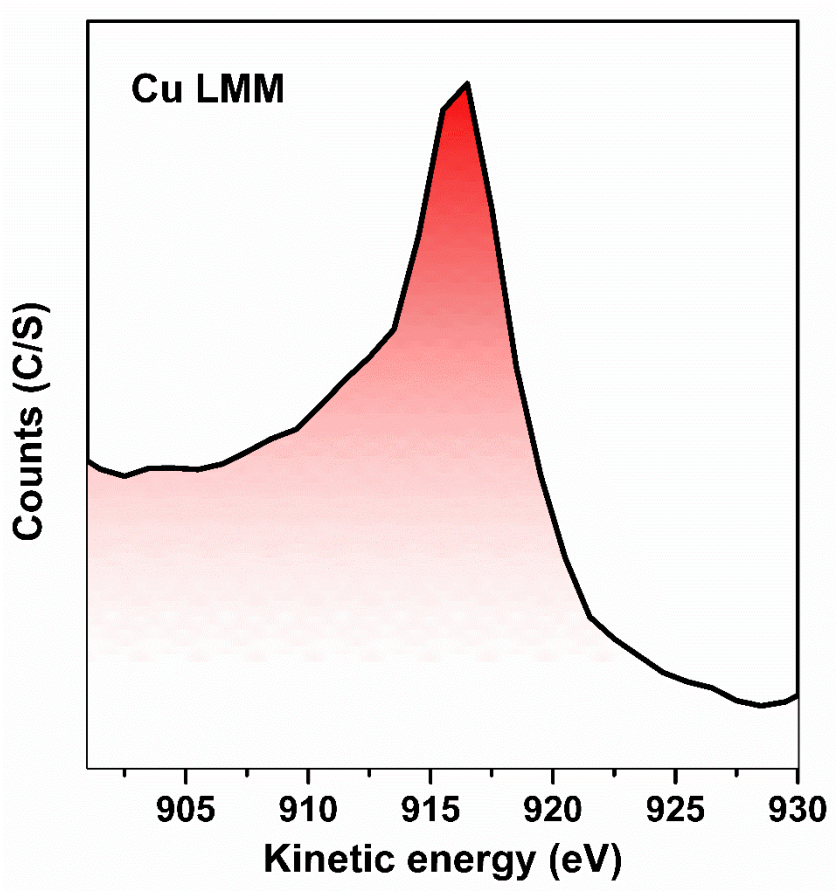

Fig. S12 Cu LMM auger spectrum of Cu_{29} NC.

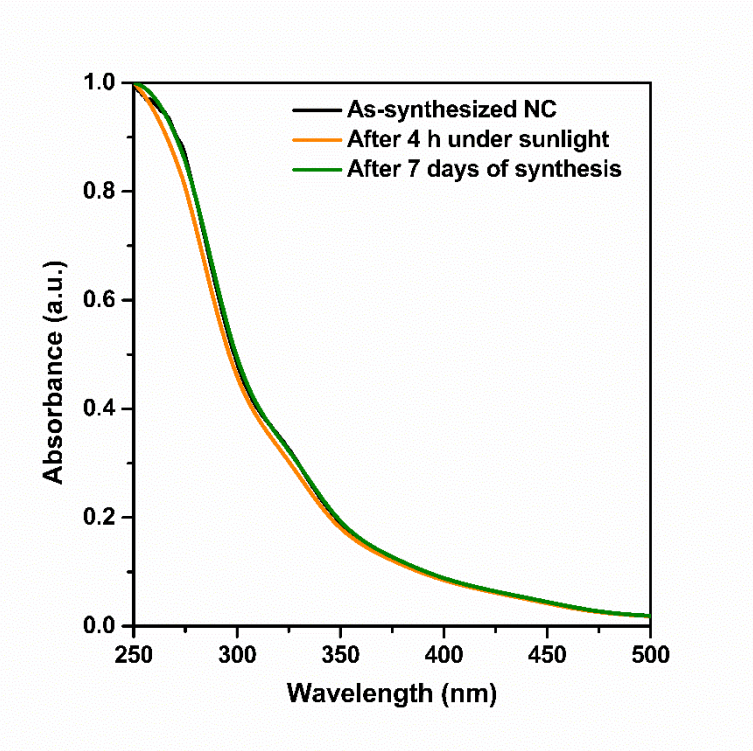

Fig. S13 Stability of as-synthesized Cu_{29} NC after exposing the crystals to sunlight for 4 hours and after 7 days keeping the crystals at ambient conditions. Note: In both the cases, before performing the absorption studies, we have dissolved the crystals in chloroform.

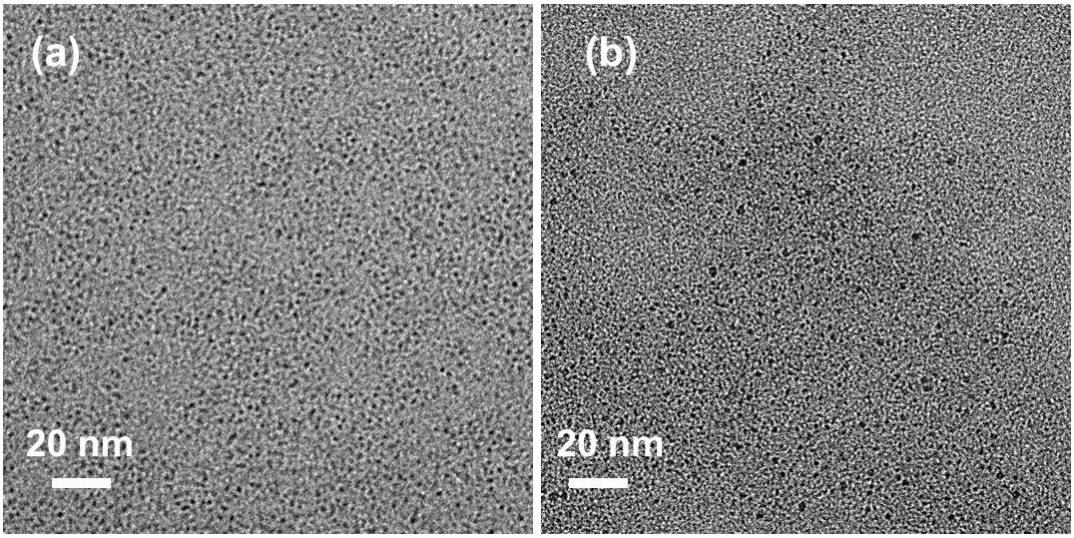

Fig. S14 TEM images of Cu_{29} NC (a) before and (b) after the catalytic reaction.

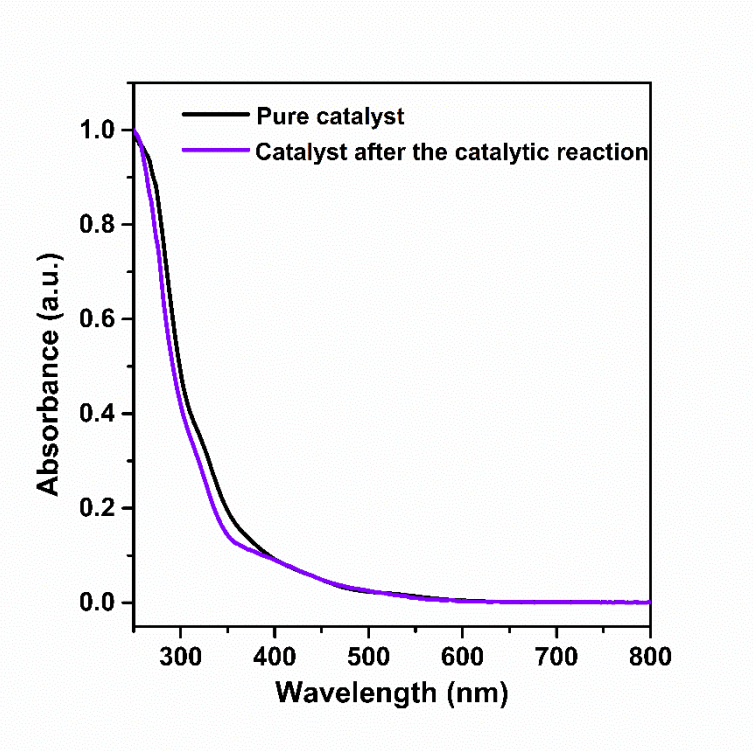

Fig. S15 Comparison of UV-vis data between the pure catalyst and isolated catalyst (after separating the catalyst from the catalytic reaction mixture) dissolved in chloroform. This suggests that the catalyst remains stable throughout the catalytic process.

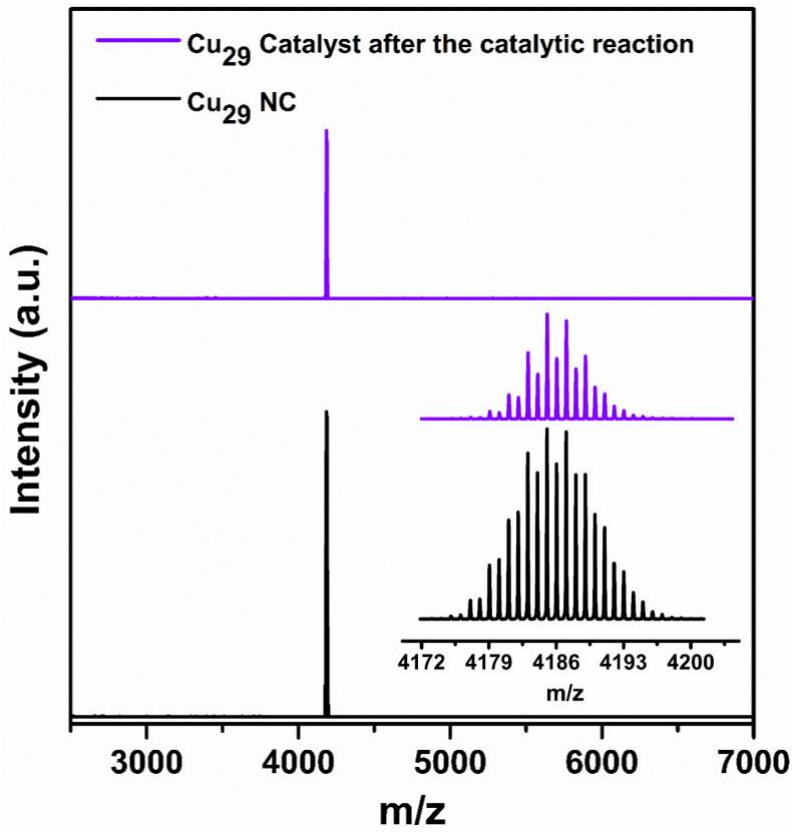

Fig. S16 Positive mode ESI-MS data of the pure catalyst and the isolated catalyst from the catalytic reaction mixture, inset shows that good overlap of the isotopic patterns between the pure catalyst and isolated catalyst.

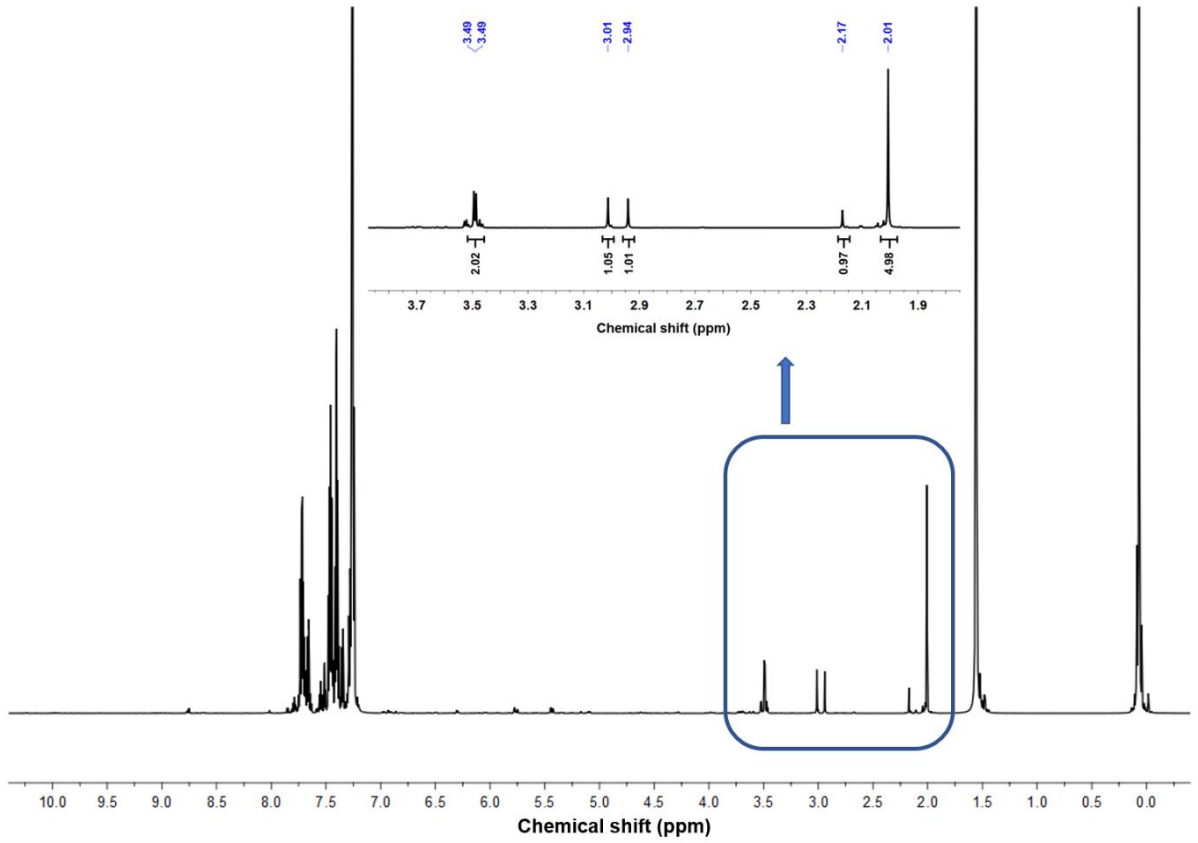

Fig. S17 ^{1}H NMR of the isolated catalyst after the catalytic reaction, inset: showing the zoomed version of the specific area which further confirmed the similar quantification of the hydrides.

NMR spectra

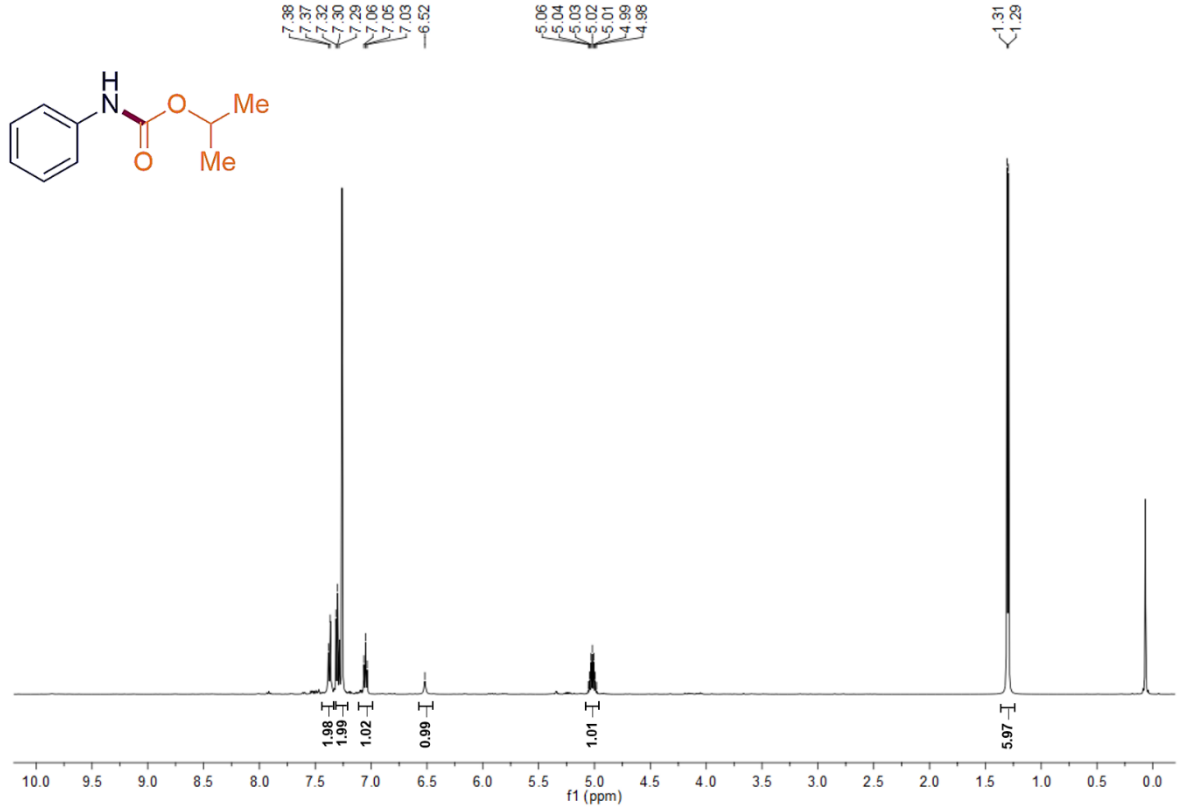

^{1}H NMR spectrum of **3aa** (500 MHz, $CDCl_3$).

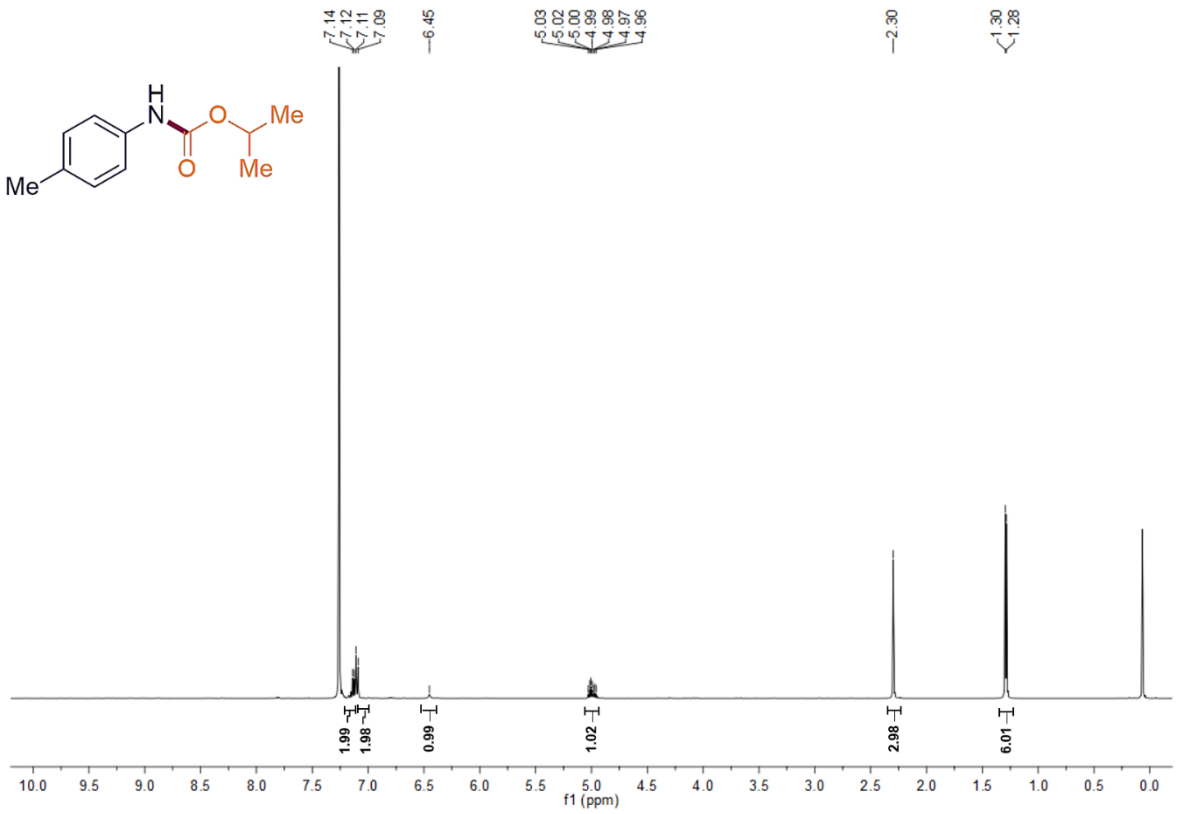

^{1}H NMR spectrum of **3ba** (500 MHz, $CDCl_3$).

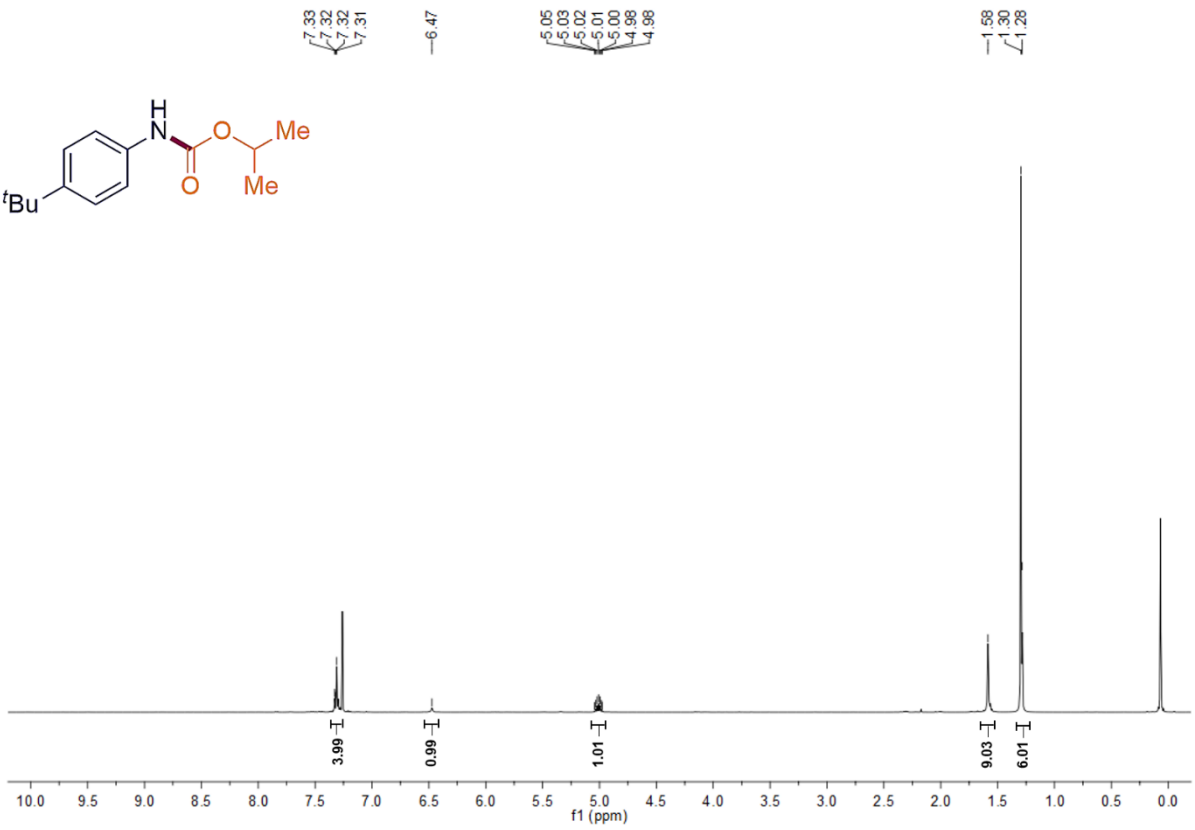

^{1}H NMR spectrum of **3ca** (500 MHz, $CDCl_3$).

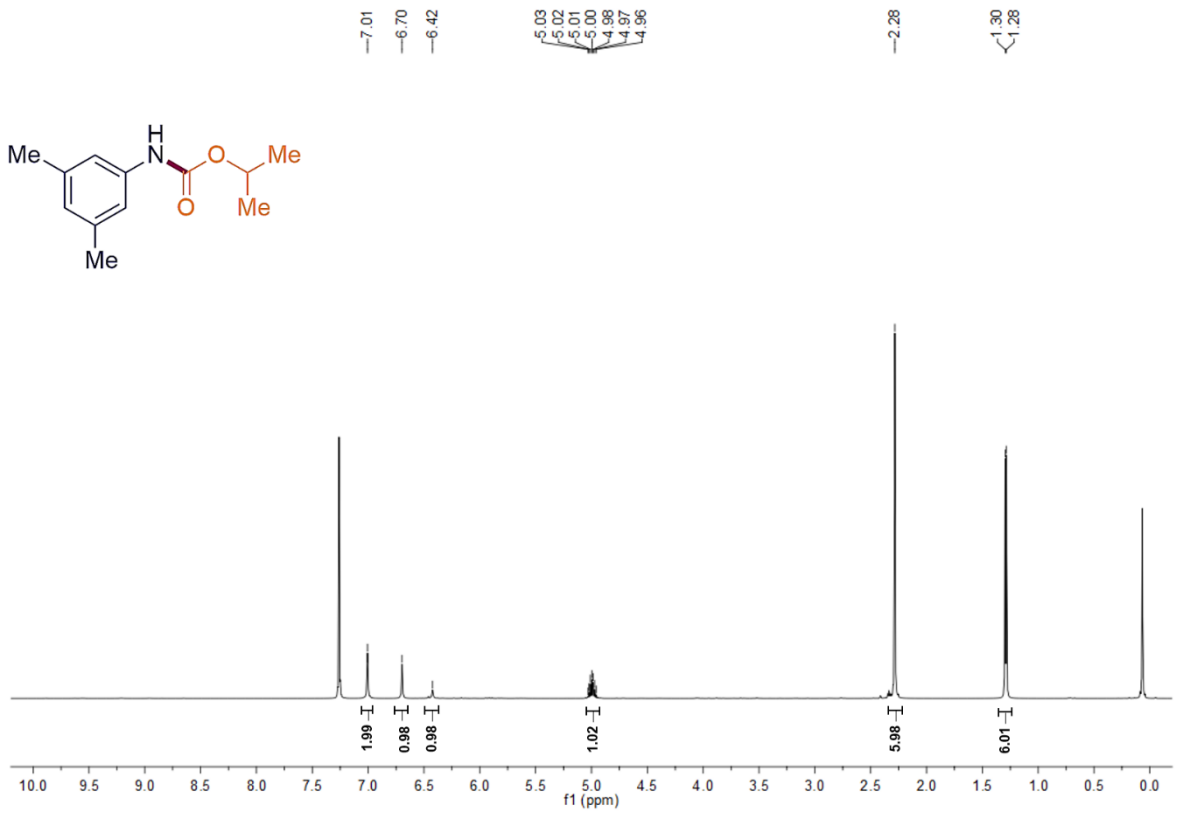

^{1}H NMR spectrum of **3da** (500 MHz, $CDCl_3$)

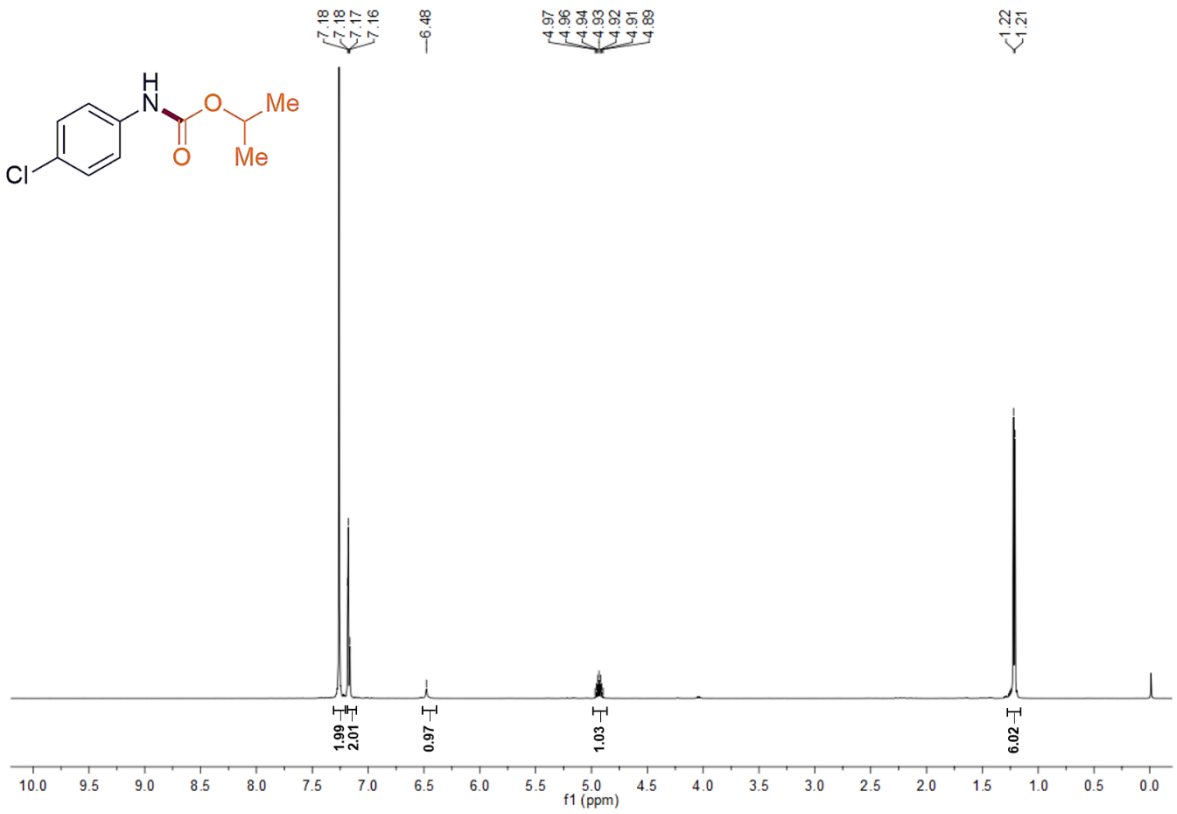

^{1}H NMR spectrum of **3ea** (500 MHz, $CDCl_3$)

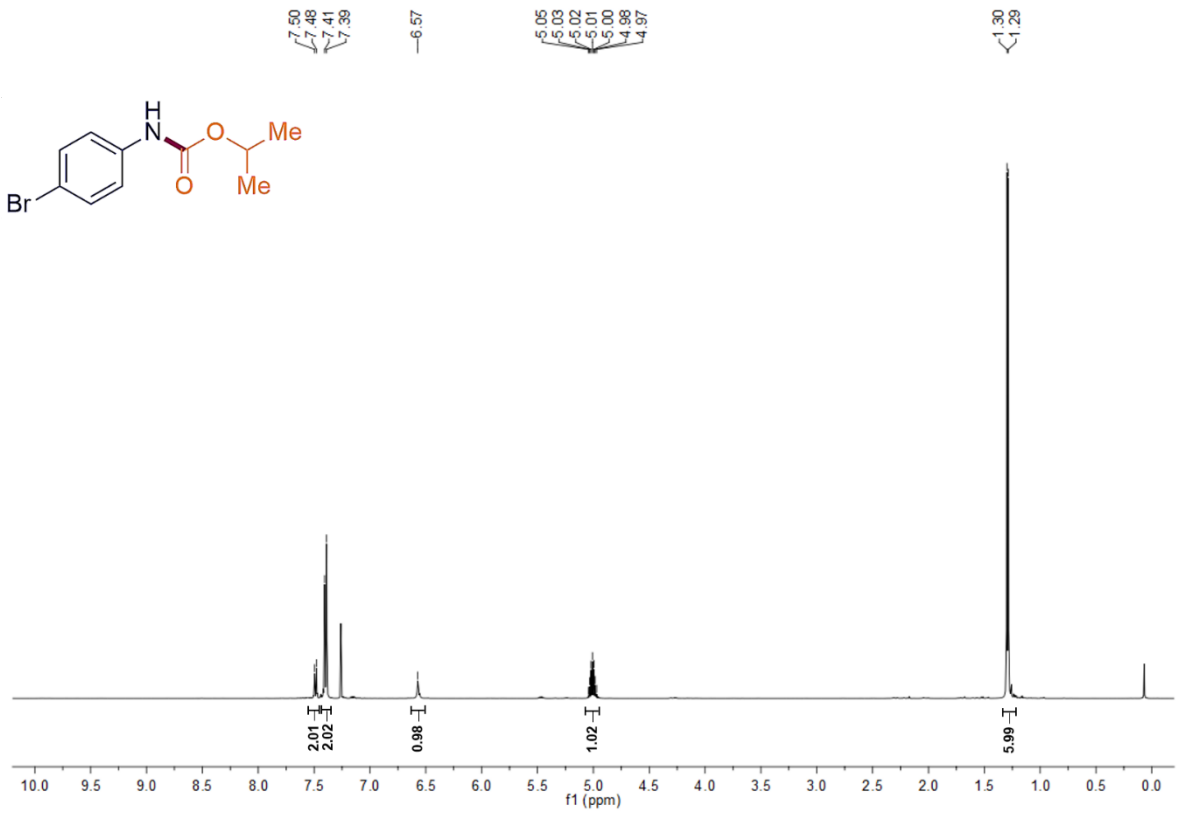

^{1}H NMR spectrum of **3fa** (500 MHz, $CDCl_3$)

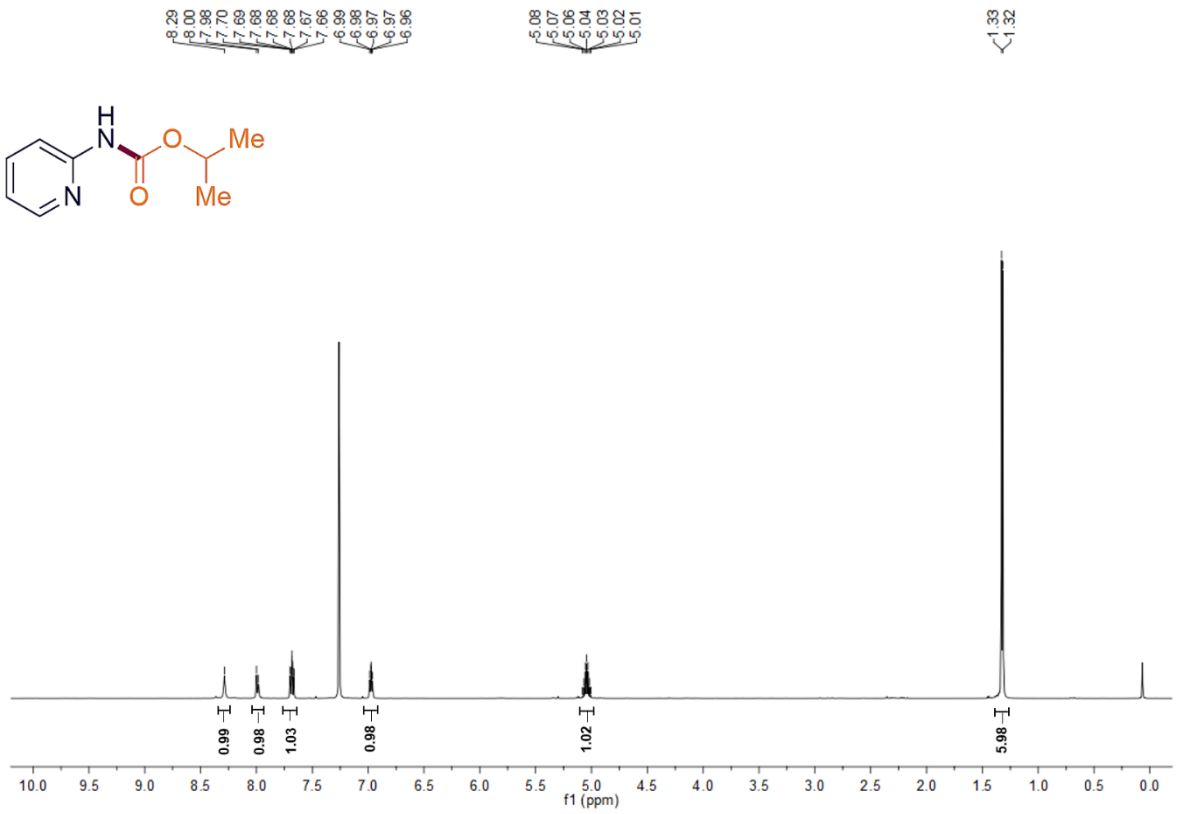

^{1}H NMR spectrum of **3ga** (500 MHz, $CDCl_3$)

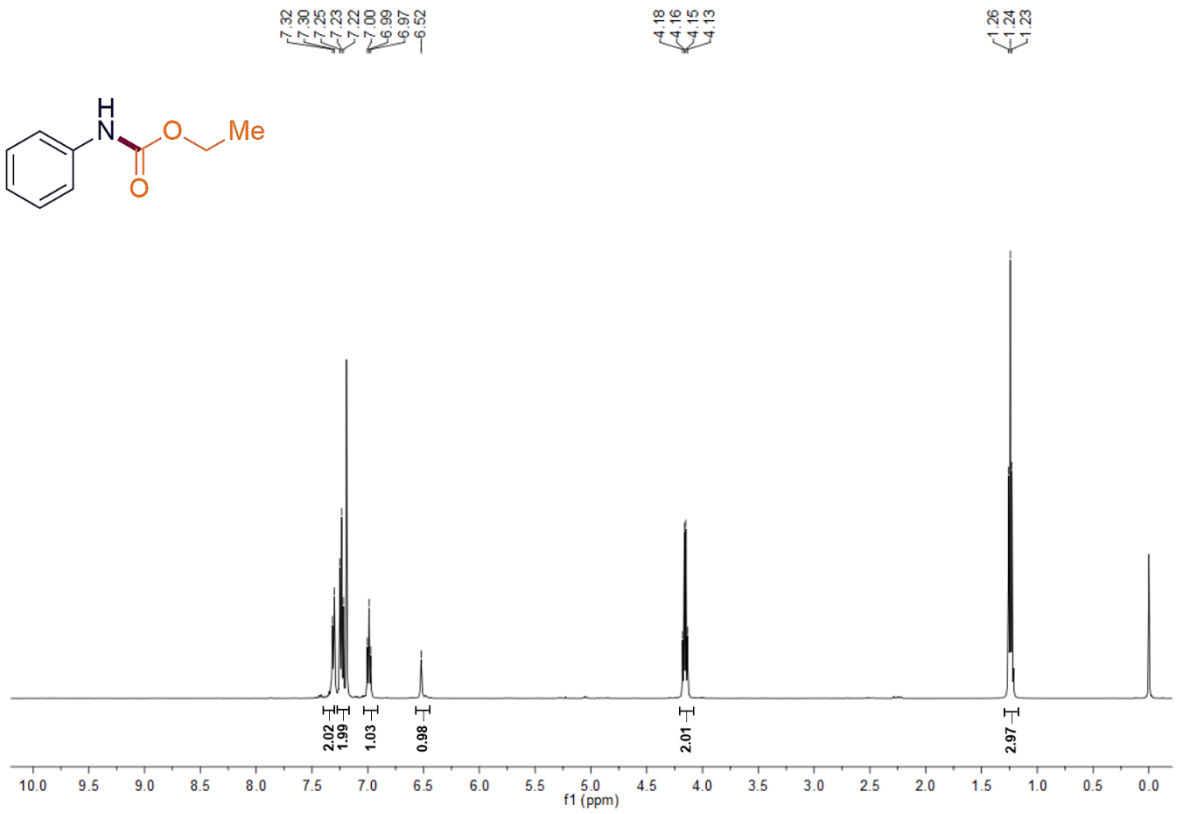

^{1}H NMR spectrum of **3ab** (500 MHz, $CDCl_3$)

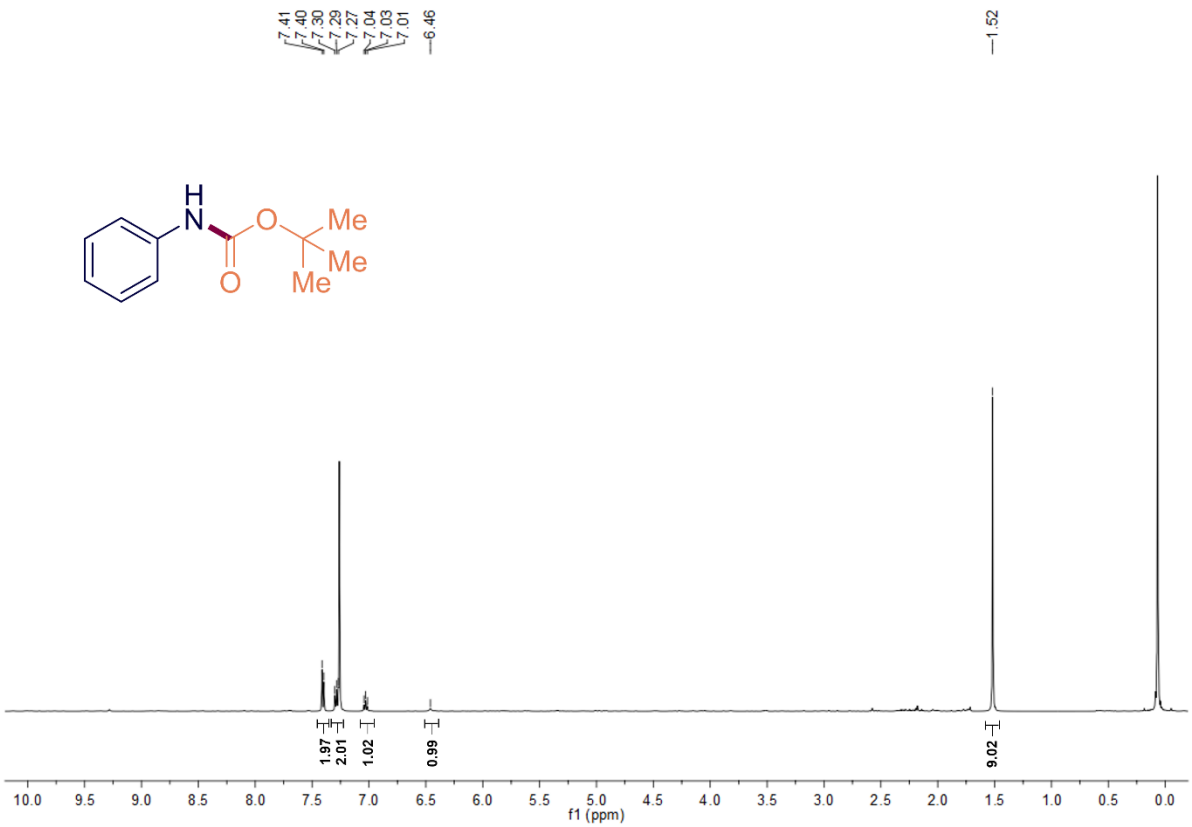

^{1}H NMR spectrum of **3ac** (500 MHz, $CDCl_3$)

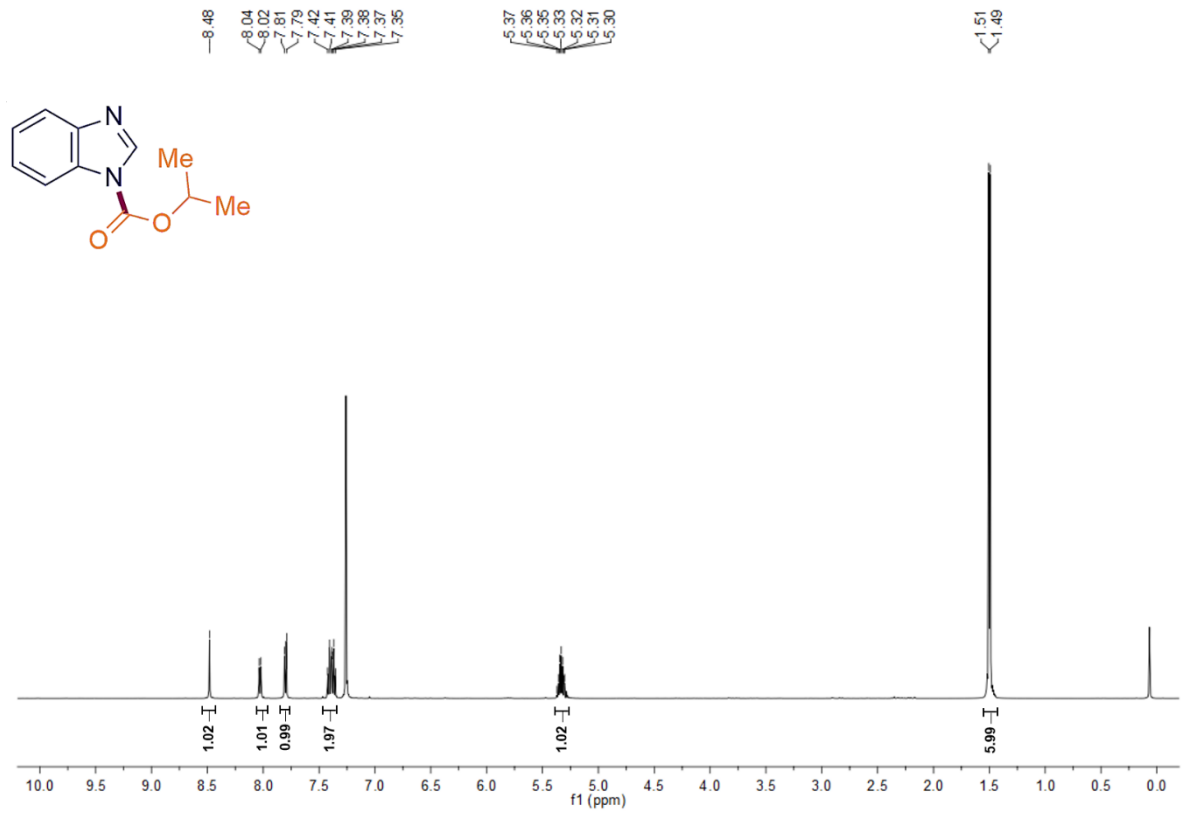

^{1}H NMR spectrum of **4a** (500 MHz, $CDCl_3$)

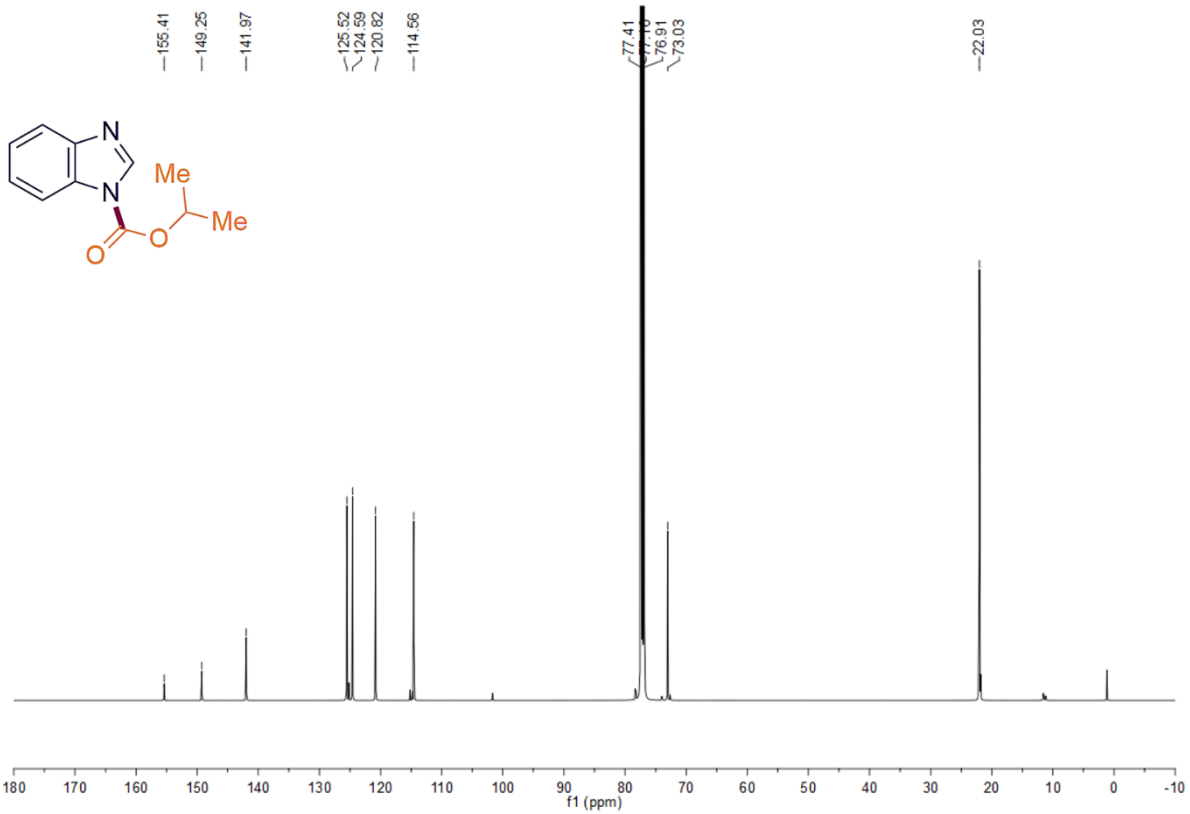

^{13}C NMR spectrum of **4a** (126 MHz, $CDCl_3$)

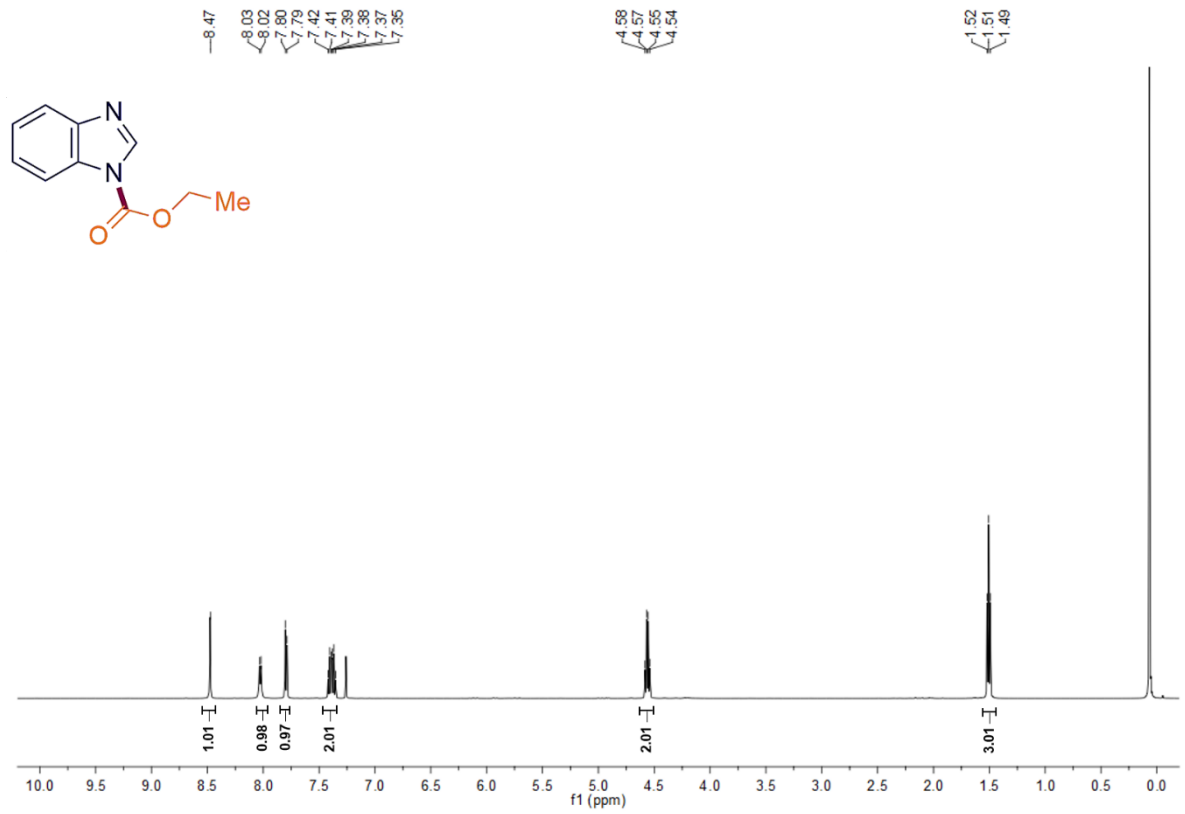

^{1}H NMR spectrum of **4b** (500 MHz, $CDCl_3$)

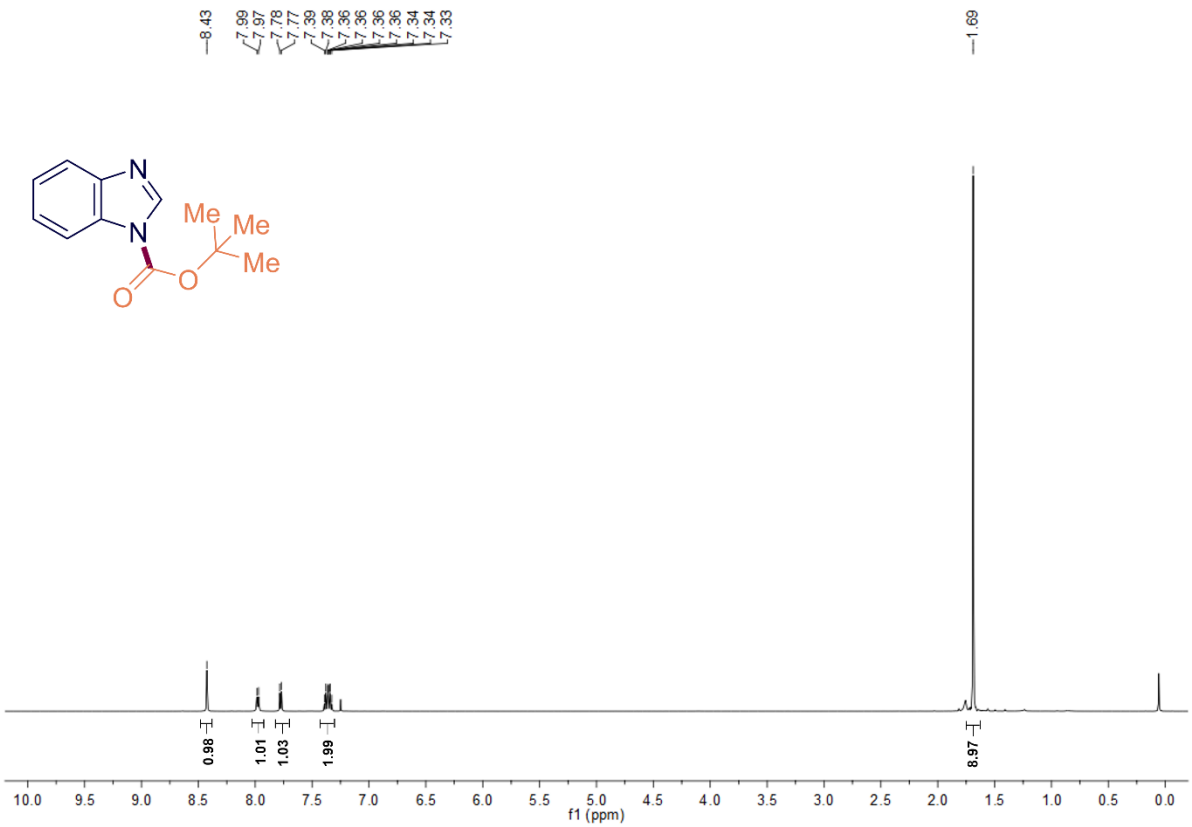

^{1}H NMR spectrum of **4c** (500 MHz, $CDCl_3$)

XYZ coordinates of the optimized structure

Cu	0.328772000000	-2.554967000000	0.596264000000
Cu	-1.408021000000	-1.460420000000	2.155710000000
Cu	-2.124666000000	-1.630052000000	-0.157130000000
Cu	0.292739000000	2.337297000000	0.345288000000
Cu	-2.112251000000	0.358012000000	-1.832008000000
Cu	2.508751000000	1.018004000000	-0.951908000000
Cu	-1.756523000000	1.020784000000	0.926799000000
Cu	1.141007000000	-3.915697000000	-4.359359000000
Cu	-2.247863000000	-3.997712000000	-1.156488000000
Cu	2.571756000000	-2.873760000000	2.228661000000
Cu	1.246839000000	-3.733960000000	-1.640904000000
Cu	3.620967000000	-1.287852000000	4.939237000000
Cu	0.207908000000	-0.191542000000	-0.313413000000
Cu	-3.347351000000	0.195325000000	2.866200000000
Cu	-3.053672000000	2.615537000000	-0.689020000000
Cu	-0.338665000000	0.069529000000	-3.994478000000
Cu	2.971789000000	1.411537000000	2.820973000000
Cu	2.843605000000	3.379032000000	0.054841000000
Cu	2.212491000000	5.191412000000	-2.601121000000
Cu	2.441990000000	-1.402933000000	-1.519268000000
Cu	2.449759000000	-0.671941000000	0.904964000000
Cu	-0.576377000000	-1.750114000000	-2.149319000000
Cu	0.459621000000	0.543155000000	2.169663000000

Cu	-0.175225000000	1.870543000000	-2.205362000000
Cu	-4.688541000000	-0.961191000000	0.174704000000
Cu	-0.915588000000	4.412684000000	-0.852632000000
Cu	-5.424419000000	2.133654000000	0.404750000000
Cu	0.272319000000	-1.231667000000	4.184045000000
Cu	2.818674000000	1.647928000000	-3.518778000000
Cl	-3.173942000000	4.920721000000	-1.099986000000
Cl	-5.532327000000	-0.759654000000	2.404765000000
Cl	-0.611263000000	-5.272088000000	-1.993702000000
Cl	4.344429000000	2.970665000000	1.887216000000
Cl	1.684918000000	0.725089000000	-5.186119000000
Cl	1.382483000000	-3.290641000000	4.321614000000
S	3.916978000000	-0.955888000000	2.707648000000
S	-0.471864000000	-2.233768000000	-4.446718000000
S	1.336058000000	0.870822000000	4.343483000000
S	1.960258000000	-4.314110000000	0.576801000000
S	0.339080000000	4.010199000000	-2.865977000000
S	-3.579029000000	2.330721000000	1.847407000000
S	0.967603000000	4.580274000000	0.577900000000
S	3.995025000000	2.594933000000	-1.852215000000
S	-4.150337000000	-3.216012000000	-0.232535000000
S	-4.462220000000	0.774144000000	-1.398974000000
S	2.939416000000	-2.875255000000	-3.195604000000
S	-2.028154000000	-0.984567000000	4.397295000000

P	-7.664093000000	1.960490000000	0.626297000000
P	4.041053000000	6.387133000000	-2.083366000000
P	1.291666000000	-6.075970000000	-5.020103000000
P	3.127525000000	-1.549561000000	7.109887000000
C	0.835472000000	-5.565562000000	1.348217000000
C	4.363366000000	-3.940963000000	-2.691805000000
C	-2.198188000000	-2.872603000000	-4.576367000000
C	-4.101298000000	-3.958026000000	1.459165000000
C	-5.506612000000	0.836432000000	-2.909610000000
C	-2.897373000000	3.922966000000	2.462498000000
C	-2.866643000000	-2.605438000000	4.711360000000
C	0.114399000000	2.131284000000	4.919232000000
C	5.629174000000	-1.045216000000	2.041777000000
C	-0.578858000000	4.306628000000	-4.430495000000
C	5.553167000000	1.695127000000	-1.422391000000
C	0.861762000000	4.660122000000	2.420257000000
C	-8.251122000000	0.327948000000	0.001423000000
C	-8.772871000000	3.170408000000	-0.211726000000
C	-8.241963000000	1.965876000000	2.373886000000
C	5.520035000000	5.965874000000	-3.091556000000
C	4.611887000000	6.160717000000	-0.348845000000
C	3.868963000000	8.210793000000	-2.257708000000
C	2.073615000000	-7.132959000000	-3.726836000000
C	2.289470000000	-6.449797000000	-6.525106000000

C	-0.307470000000	-6.929751000000	-5.348704000000
C	1.364311000000	-1.178170000000	7.481480000000
C	4.061104000000	-0.538842000000	8.331182000000
C	3.330119000000	-3.283496000000	7.688549000000
H	1.364154000000	-6.519137000000	1.419431000000
H	0.552029000000	-5.215080000000	2.341856000000
H	-0.046862000000	-5.671023000000	0.715600000000
H	4.523147000000	-4.699158000000	-3.461641000000
H	5.257668000000	-3.319663000000	-2.600578000000
H	4.148176000000	-4.422948000000	-1.736621000000
H	-2.263073000000	-3.823913000000	-4.043332000000
H	-2.873227000000	-2.150402000000	-4.111899000000
H	-2.456994000000	-3.013166000000	-5.628393000000
H	-3.114888000000	-3.794292000000	1.897420000000
H	-4.855982000000	-3.458894000000	2.068790000000
H	-4.308683000000	-5.028323000000	1.392197000000
H	-6.536718000000	1.067710000000	-2.632629000000
H	-5.118865000000	1.615260000000	-3.568946000000
H	-5.461429000000	-0.132816000000	-3.411193000000
H	-2.283543000000	3.720088000000	3.341459000000
H	-2.294682000000	4.377098000000	1.673437000000
H	-3.719332000000	4.589627000000	2.730495000000
H	-3.092757000000	-2.676805000000	5.777878000000
H	-3.789651000000	-2.639390000000	4.130493000000

H	-2.205208000000	-3.422024000000	4.416701000000
H	-0.225107000000	1.837932000000	5.915023000000
H	0.598202000000	3.108111000000	4.961016000000
H	-0.735932000000	2.157104000000	4.236650000000
H	5.564800000000	-0.921012000000	0.959366000000
H	6.218195000000	-0.237830000000	2.479999000000
H	6.065282000000	-2.014306000000	2.287824000000
H	-1.575342000000	3.877041000000	-4.311782000000
H	-0.652413000000	5.378499000000	-4.621954000000
H	-0.055196000000	3.805843000000	-5.247431000000
H	6.376540000000	2.124729000000	-1.996651000000
H	5.719565000000	1.829178000000	-0.351989000000
H	5.435638000000	0.635954000000	-1.652321000000
H	0.878068000000	5.707118000000	2.730911000000
H	-0.058450000000	4.180666000000	2.747886000000
H	1.721495000000	4.128123000000	2.833424000000
H	-0.488406000000	1.884430000000	1.821669000000
H	-1.489254000000	1.810873000000	-0.723520000000
H	-1.371099000000	1.178159000000	-3.267336000000
H	-2.216761000000	-1.400559000000	-1.871974000000
H	0.721711000000	-1.774988000000	-1.083635000000
H	3.436278000000	-0.408099000000	-0.519768000000
H	0.829099000000	-0.976646000000	1.461011000000
H	-1.256583000000	-2.835375000000	1.105408000000

H	-2.577533000000	-0.470006000000	1.067696000000
H	0.876852000000	1.287763000000	-0.957612000000
H	-9.312701000000	0.177583000000	0.226207000000
H	-7.657019000000	-0.457968000000	0.476972000000
H	-8.099642000000	0.271386000000	-1.080410000000
H	-9.825893000000	2.921699000000	-0.039619000000
H	-8.571039000000	3.163901000000	-1.287438000000
H	-8.571430000000	4.175155000000	0.172451000000
H	-7.683628000000	1.198885000000	2.918686000000
H	-9.315700000000	1.757013000000	2.435813000000
H	-8.032893000000	2.941137000000	2.824411000000
H	6.394699000000	6.531619000000	-2.753577000000
H	5.321862000000	6.195807000000	-4.142796000000
H	5.717305000000	4.893907000000	-2.999337000000
H	5.446070000000	6.835256000000	-0.128319000000
H	4.938304000000	5.126718000000	-0.204074000000
H	3.784564000000	6.355866000000	0.339426000000
H	3.602754000000	8.455811000000	-3.290182000000
H	4.804959000000	8.714505000000	-1.993926000000
H	3.069950000000	8.562735000000	-1.598142000000
H	2.094796000000	-8.184901000000	-4.032305000000
H	1.507472000000	-7.031229000000	-2.796719000000
H	3.095933000000	-6.786700000000	-3.547081000000
H	2.321186000000	-7.528262000000	-6.716711000000

H	3.309037000000	-6.076572000000	-6.386721000000
H	1.849145000000	-5.942321000000	-7.388998000000
H	-0.942850000000	-6.834247000000	-4.463681000000
H	-0.150361000000	-7.989532000000	-5.577632000000
H	-0.809442000000	-6.446694000000	-6.192854000000
H	1.153339000000	-1.347698000000	8.542723000000
H	0.729160000000	-1.828750000000	6.873113000000
H	1.144766000000	-0.140048000000	7.219293000000
H	3.718345000000	-0.749032000000	9.349834000000
H	3.912472000000	0.522789000000	8.111329000000
H	5.128696000000	-0.765688000000	8.253476000000
H	2.738694000000	-3.934660000000	7.038211000000
H	2.992072000000	-3.390754000000	8.724650000000
H	4.382199000000	-3.575254000000	7.616417000000

References

S1. O. V. Dolomanov, L. J. Bourhis, R. J. Gildea, J. A. Howard and H. Puschmann, *J. Appl. Crystallogr.*, 2009, **42,** 339-341.

S2. G. M. Sheldrick, *Acta Crystallogr. Sec. C: Struc. Chem.*, 2015, **71,** 3-8.

S3. G. M. Sheldrick, *Acta Crystallogr. Sec. A: Found. Adv.*, 2015, **71,** 3-8.

S4. A. L. Spek, *Acta Crystallogr. Sec. C: Struc. Chem.*, 2015, **71,** 9-18.

S5. C. Dong, R.-W. Huang, C. Chen, J. Chen, S. Nematulloev, X. Guo, A. Ghosh, B. Alamer, M. N. Hedhili, T. T. Isimjan, Y. Han, O. F. Mohammed and O. M. Bakr, *J. Am. Chem. Soc.*, 2021, **143,** 11026-11035.

S6. J. P. Perdew, J. A. Chevary, S. H. Vosko, K. A. Jackson, M. R. Pederson, D. J. Singh and C. Fiolhais, *Phys. Rev. B*, 1992, **46,** 6671.

S7. G. Kresse and J. Furthmüller, *Comput. Mater. Sci.*, 1996, **6,** 15-50.

S8. G. Kresse, J. Furthmüller and J. Hafner, *Phys. Rev. B*, 1994, **50,** 13181.

S9. P. E. Blöchl, *Phys. Rev. B*, 1994, **50,** 17953.

S10. M. Frisch, G. Trucks, H. Schlegel, G. Scuseria, M. Robb, J. Cheeseman, G. Scalmani, V. Barone, B. Mennucci and G. Petersson, *Wallingford, CT* 2009, **32,** 5648-5652.

S11. A. D. Becke, *J. Chem. Phys.*, 1993, **98,** 5648-5652.

S12. A. McLean and G. Chandler, *J. Chem. Phys.*, 1980, **72,** 5639-5648.

S13. P. J. Hay and W. R. Wadt, *J. Chem. Phys.*, 1985, **82,** 270-283.

S14. W. R. Wadt and P. J. Hay, *J. Chem. Phys.*, 1985, **82,** 284-298.

S15. M. Usman, Z.-H. Ren, Y.-Y. Wang and Z.-H. Guan, *RSC Adv.*, 2016, **6,** 107542-107546.

S16. N. V. Reddy, K. R. Prasad, P. S. Reddy, M. L. Kantam and K. R. Reddy, *Org. Biomol. Chem.*, 2014, **12,** 2172-2175.

S17. N. Uhlig and C. J. Li, *Chem. Eur. J.*, 2014, **20,** 12066-12070.

S18. S. Majumdar, J. De, A. Chakraborty and D. K. Maiti, *RSC Adv.*, 2014, **4,** 24544-24550.